

ANALYSIS OF SEMICONDUCTOR LASER-TRANSMITTER MODEL BASED ON TRANSMISSION-LINE LASER MODELLING

Master of Science Thesis

Aigerim Nurbayeva 1380292 <u>axn392@bham.ac.uk</u>

Supervisor: Dr. H. Ghafouri-Shiraz

School of Electronic, Electrical and Computer Engineering

College of Engineering and Physical Sciences

The University of Birmingham

03 September 2014

Abstract

The present thesis reports the results of a simulation of a one-dimensional laser model by using transmission-line laser modelling (TLLM) technique in Matlab environment. It introduces a literature review of laser modelling approaches, basic optical processes within a laser, a general transmission line theory and the transmission-line matrix method.

Implementation of TLLM algorithm is explained in detail. The simulation of the model takes into account as physical as optical parameters of the laser. For instance, it considers electrical parasitics and matching circuit part; carrier and photon density, refractive index change, spontaneous emission etc.

All results are simulated in time domain first and converted in frequency domain independently by using Fast Fourier Transform (FFT). Several simulation results as return loss, optical power are presented.

Finally, analysis of the relevance of the TLLM technique is discussed. The future work of improving the obtained results is proposed.

Acknowledgement

First of all, I would like to thank Dr. Hooshang Ghafouri-Shiraz for involving me in such fascinating, not daily project. For his constant support and inspiration, that has not given me up during the dissertation. For his contribution in fiber optic communication by releasing series of books and articles that are always shown in detailed and understanding manner, which helps me so much, especially in my particular research area.

Secondly, I appreciate Kazakhstan government for developing education system in my country and granting me scholarship that made possible my learning at Master's degree.

Lastly, I would like to express my great love and respect to my mother Zure who always try to give me the best of this life and inspires me in everything. I'm also grateful of all my friends for being in my life and doing it easier.

Contents

Introduction	1
1 Literature review	3
2 Background	5
2.1 Transmission-Line Matrix Method	5
2.2 Laser Diode	7
2.2.1 Radiative Processes	7
2.2.2 Recombination Processes	8
2.2.3 Population Inversion and Optical Gain	9
3 Methodology	11
3.1 Equivalent circuit of semiconductor laser based on lumped elements	11
3.1.1 RF source	12
3.1.2 Intrinsic laser	12
3.1.3 Electrical parasitics	13
3.1.4 Matching network	14
3.2 The TLLM algorithm	20
3.3 The TLLM method of physical parameters of the laser	20
3.3.1 TLM link and stub modelling	20
3.3.2 The laser-transmitter model based on TLLM	22
3.3.3 Scattering and connecting process	24
3.4 The TLLM method of optical processes inside the laser-transmitter	26
3.4.1 Carrier density model	27
3.4.2 Amplification Model	28
3.4.3 Laser Chirp Modelling	31

3.4.4 Spontaneous emission model	33
3.5 Laser's parameters	34
4 Results and Discussion	36
4.1 Return loss	37
4.2 Large signal analysis	38
5 Conclusion	41
References	42
Appendix A	47
Appendix B	48

List of figures

- Figure 1.1 Huygens's principle in Cartesian mesh.
- Figure 1.2 Scattering process.
- Figure 1.3 Energy state diagram of fundamental processes.
- Figure 1.4 Populations in a two energy level systems.
- Figure 1.5 Schematic of semiconductor laser structure.
- Figure 3.1 Equivalent circuit of semiconductor laser.
- Figure 3.2 The schematic cross section of the ridge waveguide laser.
- Figure 3.3 L-section matching network.
- Figure 3.4 L-section matching network for frequencies below (a) and at (a) 6.6 GHz implemented in AWR microwave office.
- Figure 3.5 Return loss (S11 parameter).
- Figure 3.6 Smith chart.
- Figure 3.7 Matching network.
- Figure 3.8 TLM link-lines.
- Figure 3.9 TLM stub-lines.
- Figure 3.10 The equivalent laser-transmitter model based on TLLM.
- Figure 3.11 The TLLM considering optical process.
- Figure 3.12 The equivalent circuit of the carrier density rate equation.
- Figure 3.13 Block diagram of the gain filter.
- Figure 3.14 The TLM stub filter.
- Figure 3.15 Stub- attenuator model.
- Figure 3.16 Presentation of one section of distributed spontaneous emission model
- Figure 4.1 Signal from sinusoidal generator

- Figure 4.2 Signal from rectangular generator
- Figure 4.3 S11 parameter for 1.1GHz and 6.6GHz respectively
- Figure 4.4 Gain-switched optical pulses over 20psec
- Figure 4.5 Stable averaged optical pulse
- Figure 4.6 Optical spectrum when gain-switched with linewidth enhancement factor equal 0
- Figure 4.7 Optical spectrum when gain-switched with linewidth enhancement factor equal 5.6

List of tables

- Table 3.1 Parameters of the equivalent circuit
- Table 3.2 The values of the reactive elements of the L-section matching network
- Table 3.3 Parameters of the laser

Acronyms and abbreviations

LD - laser diodes;
LED - light-emitting diodes;
TLM - Transmission-Line Matrix;
TLMM - Transmission-Line Matrix Method;
TMM - Transfer Matrix Model;
TDM - Time-Domain Model;
PMM - Power Matrix Model;
DFB laser - Distributed feedback laser;
TLLM - Transmission-Line Laser Model;
FFT - Fast Fourier Transform;

Introduction

An optical fiber communication system has become widely spread due to several well-known beneficial features including greater bandwidth, immunity to electromagnetic interference, low losses over long distances and data security [1].

In such systems, an optical source performs one of the main functions of the transmitter. Generally, light source can be presented by two relevant sources such as laser diodes (LDs) and light-emitting diodes (LEDs), however further discussion will regard the laser diode only.

Over the years the researchers have worked to improve of laser diode parameters, as a consequence it has high efficiency, sufficient output power, good reliability and small size [2]. In spite of this, investigation for further improvement of the laser's characteristics continues. Mainly, progress is directed to the research area of 'stable single frequency operation, high output power and increasing direct modulation bandwidth' [3]. Hence, in order to evaluate the laser performance different approaches of laser modelling have been suggested.

Modelling is a flexible and efficient stage in designing of any device. Usually modelling and simulation processes exist to understand and predict the operation, behavior of the device and factors influencing them. Therefore, the modification or optimization of the model in order to achieve better results does not affect the economic aspects as seriously as the fabrication of the device again.

Considering above, the analysis of semiconductor laser transmitter model based on TLLM is provided. The modelling method in the project is chosen as the TLLM has several advantages over other methods (different laser modelling methods will be discussed in Literature Review section). Firstly, TLLM has an ability to consider different types of laser structures. Secondly, the method allows taking into account important effects occurring in the laser, which significant influence to the laser performance such as carrier-induced refractive index change, random spontaneous emission noise, reflections and optical phase information не вижу глагола в этом придаточном предложении. Могеоver, resulting simulation of laser can involve matched an unmatched case [3].

Generally, the proposed laser model is intended for the range of microwave signal. With this purpose, the general idea of microwave-optoelectronic model based on article by Sum and Gomes [4] is applied. However, the proposed model was upgraded by Wong and Ghafouri-Shiraz [5] by matching the signal source and laser and by representing an integrated model, including matching network, electrical parasitics and intrinsic laser together.

It is important to note, that the present thesis follows the main research paper by Wong and Ghafouri-Shiraz [5]. Nonetheless, the project is considered as deep exploration of the theory applied in the article and the simulation of the proposed model in Matlab environment. As a consequence, a detailed analysis will be produced.

The thesis is organized as follows. First, in a Literature review section different laser modelling approaches are briefly presented, which have been evaluated and improved over the years. Theoretical basis required for clear understanding of the main objective of the project and further investigation is described in a Background section. Methodology section contains all information about implementation of laser based on TLLM and resulting model itself. All simulation tests of the model taken under the given parameters are presented in Results section. Finally, analysis of the achieved results and summary of the project are shown in a Discussion and Conclusion sections respectively.

1 Literature review

During the active development of optical fiber technologies various methods of laser modelling have been proposed. Several of them are discussed in this section.

The idea of the Transmission-Line Laser Modelling originates from the Transmission-Line Matrix Method (TLMM) which is applied for passive waveguides [6,7,8]. In the research article suggested by Johns [6] a numerical solution of scattering problems using a TLMM is presented. The main point of the work is to calculate the wave impedances in a waveguide by different ways. The obtained results in the article demonstrate that TLMM is in a good agreement with the numerical method.

Another substantial work performed by Akhtarzad [7] is dedicated to analysis of microwave structures and microwave resonators by using two and three dimensional TLMM. The authors achieved many different outcomes for resonators, homogeneous and inhomogeneous waveguides with different conditions, supporting all calculation by programming in FORTRAN language. The results also show a high accuracy of the TLMM despite the fact that some errors are taken into account.

Based on above and other sources, the theory and applications of TLMM are discussed by Hoefer [8] in his resulting review. Some of the theory of this research work will be explained in Background chapter for a good understanding of the fundamentals of Transmission-Line Laser Modelling.

Meanwhile, the semiconductor laser's researchers have been investigating several models which general purpose is to solve the carrier density and photon density rate equations [9]. Among them the coupled-cavity laser model proposed by Marcuse [10]. According to the work, a derivation of rate equations for the special case is shown in order to analyze the performance of the coupled-cavity laser.

A detailed description of field equations used in simulation and brief discussion of various methods (including a Galerkin's method, direct integration, finite difference) for solving them are published by Buus [11]. Moreover, an overview of static and dynamic laser models is also presented.

One of the publications suggested a different way for designing semiconductor laser by using a special simulator made by Ohtoshi et al [12]. The developed tool named HILADIES (Hitachi Laser Diode Engineering Software) is intended to compute equations for electrons

and holes. The current and voltage characteristics were also carried out. It is shown that presented model is valid with comparing the numerical results.

As a result a large number of scientific publications have been released, however little of them considered a complex structure and processes occurring inside of semiconductor laser. Therefore, new works have been aimed to perform more complete and realistic model. It can be obtained by combining a solution of rate equations and wave propagation in a model at the same time [9].

All these conditions can be met in the following laser models: transfer matrix model (TMM), Time-Domain Model (TDM), and Power Matrix Model (PMM) [3].

Bjork et. al. provided analyses of one-dimensional asymmetric phase-shifted Distributed Feedback (DFB) *Laser* structures by using transfer matrix method [13]. The algorithm is presented as follows. The laser model is divided for a finite number of discrete parts, each of them represented by transfer matrix. Then, the overall transfer matrix of the separated parts of the model is calculated in order to describe the wave propagation along the cavity and obtain a power output characteristic. The main advantage of the model is that it can be used for different laser structures. Further work by Davis et.al. [14] suggested simulating dynamic TMM (e.g. analyze each section of the model individually depending on time, which leads to renewal of parameters of the wave propagating through the sections).

A dynamic response of DFB laser by using Power Matrix Model (PMM) is proposed by Zhang et.al. [15]. The one dimensional model is designed to represent the field equation to power equation, taking into account important parameters of laser such as carrier and photon density, carrier induced index change, the spontaneous coupling factor. Moreover, the time-dependent model divided by sections can consider inhomogeneous structure overall as each section can evaluate its own uniform distribution. As a result, the model can show different characteristics depending on laser cavity.

According to TDM, the number of complex numerical equation should be solved in order to obtain a travelling-wave equation, which carries information about operation and processes of semiconductor laser [16].

Lastly, the Transmission-Line Laser Model well presented in series publication by Lowery provoked many research articles that describe implementation of this model on different types of laser. This model will be discussed in detail during this dissertation [17].

2 Background

Analysis conducted in this thesis is supported by the following basic theory, which may be useful for introducing the principles, approaches and details related with the main concept. Therefore, the fundamental idea of laser diode and Transmission-Line Matrix Method are briefly reviewed.

2.1 Transmission-Line Matrix Method

The main purpose of developing the Transmission-Line Matrix Method (TLMM) is an analysis of wave propagation in a time domain. In order to explain this concept Hoefer [8] refer to the Huygen's principle statement, which interpreted as follows [18]:

'Every point on a wave front can be considered as a new source of spherical wavelets'.

The representation of the Huygen's principle in discrete form can be modelled by Cartesian mesh of nodes, where the finite parameters of mesh can be defined as [8]:

$$\Delta t = \Delta l / c \,, \tag{1.1}$$

where Δt - unit of propagation time from one node to the next;

 Δl - unit of separated distance between nodes;

c - speed of light.

The propagation algorithm in a mesh is described as follows. Initially, the Dirac voltage-impulse incident to the node from the negative side, then the energy unit of that incident pulse is scattered uniformly in all four directions as depicted in Figure 1.1 [8]. It is important to note, that all four branches are identical, therefore the reflection coefficient is equal -1/2, as a consequence the reflected impulse is also negative [8].

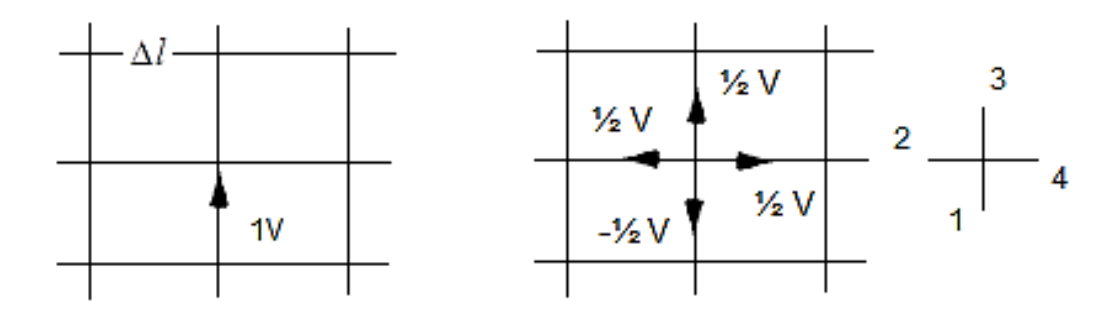


Figure 1.1 – Huygens's principle in Cartesian mesh.

For instance, when four pulses incident to four adjacent branches, the overall voltage of reflected impulse can be determined as [8]:

$${}_{k+1}V_n^r = \frac{1}{2} \cdot \left[\sum_{m=1}^4 {}_k V_m^i \right] - {}_k V_n^i \,, \tag{1.2}$$

where $_{k}V_{n}^{i}$ - incident voltage pulse on the 1-4th branches at time $t = k \cdot \Delta t$;

 $_{k+1}V_n^r$ - total reflected voltage pulse at time $t=(k+1)\cdot \Delta t$.

The relation between the incident and reflected pulses can be explained by scattering matrix equation [8]:

$$\begin{pmatrix} V_1 \\ V_2 \\ V_3 \\ V_4 \end{pmatrix}^r = 1/2 \cdot \begin{pmatrix} -1 & 1 & 1 & 1 \\ 1 & -1 & 1 & 1 \\ 1 & 1 & -1 & 1 \\ 1 & 1 & 1 & -1 \end{pmatrix} \cdot \begin{pmatrix} V_1 \\ V_2 \\ V_3 \\ V_4 \end{pmatrix}^i$$

$$(1.3)$$

Another relation occurs between the adjacent nodes. It is described as follows. The reflected pulse from one node is equal to the incident pulse of the neighboring node (formula 1.4)

$$V_1^i(z,x) = V_3^r(z,x-1)$$

$${}_{k+1}V_2^i(z,x) = {}_{k+1}V_4^r(z-1,x)$$
(1.4)

$$V_{k+1}^{i}V_{3}^{i}(z,x)=V_{1}^{r}(z,x+1)$$

$$_{k+1}V_4^i(z,x) = _{k+1}V_2^r(z=1,x)$$

As a result, if the incident voltage of the one node is known the other reflected voltage of this node or the reflected voltage of the previous node can be defined.

These two relations (formula 1.3, 1.4) mentioned above are formed the basis of Transmission-Line Matrix Method.

The following Figure 1.2 [8] shows the example of wave propagation in two-dimensional mesh by injecting a Dirac voltage-impulse.

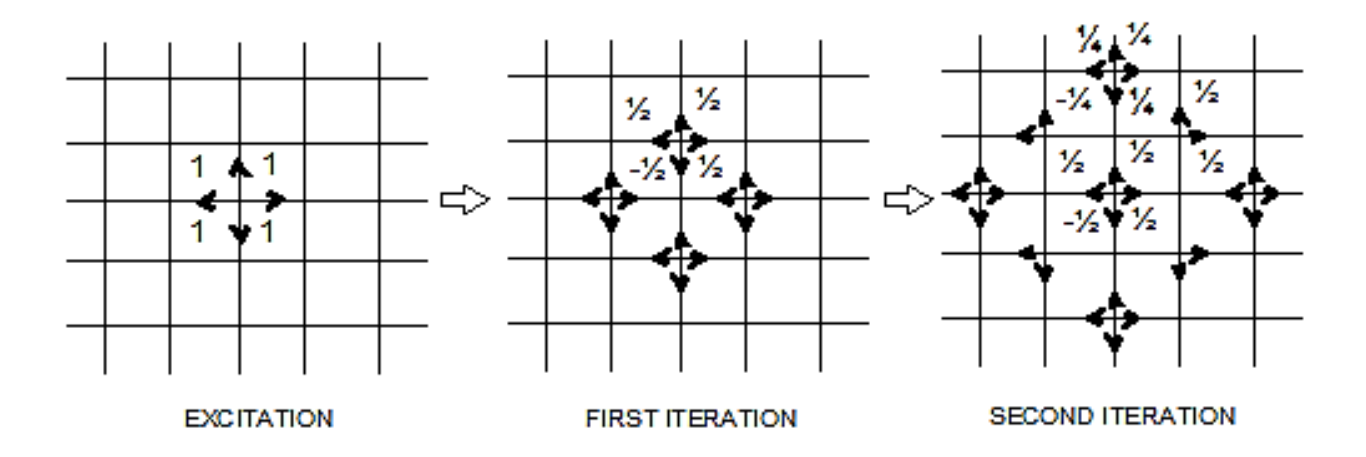


Figure 1.2 – Scattering process.

2.2 Laser Diode

Laser Diode is a type of a light source, which designed to transfer electrical energy to optical analogue. There are several types of laser diode such as solid-state lasers (ruby laser etc.), gas lasers (helium laser etc.) and semiconductor lasers. In this thesis semiconductor laser is used and will be discussed further.

2.2.1 Radiative Processes

According to quantum theory, the physical processes occurring inside the laser is due to transition of atoms from one energy state to another. Hence, the difference of energy is defined as: $E=E_2-E_1=hf$, where $h=6.626\cdot 10^{-34}\,J$ is a Plank's constant. Moreover, alteration of energy state is accompanied by absorption and emission of radiation, where the last is divided into two types: spontaneous emission and stimulated emission. These fundamental processes are depicted in a figure 1.3 [1] and can be described as follows [1]. There are two energy states E₁ and E₂ corresponding to the ground and the excited state of atoms. Initially, an atom most often is in the lower state, because it is more stable at this level. By assuming existence of incident photon with energy (E₂-E₁), it is a high chance that an atom will change ground energy state to the excited state by absorption of energy (fig.1.3 a). On the other hand, transition of an atom from higher energy level to lower takes place by emission of energy. Herewith the spontaneous emission is a consequence of emission of random photons without phase relationship between them, e.g. incoherent radiation (fig. 1.3 b). Regarding the stimulated emission, it occurs by initiating of existing photon and as a result a new created photon is of identical energy, in phase and same polarization with the incident one, e.g. coherent radiation (fig.1.3 c) [1, 2, 3].

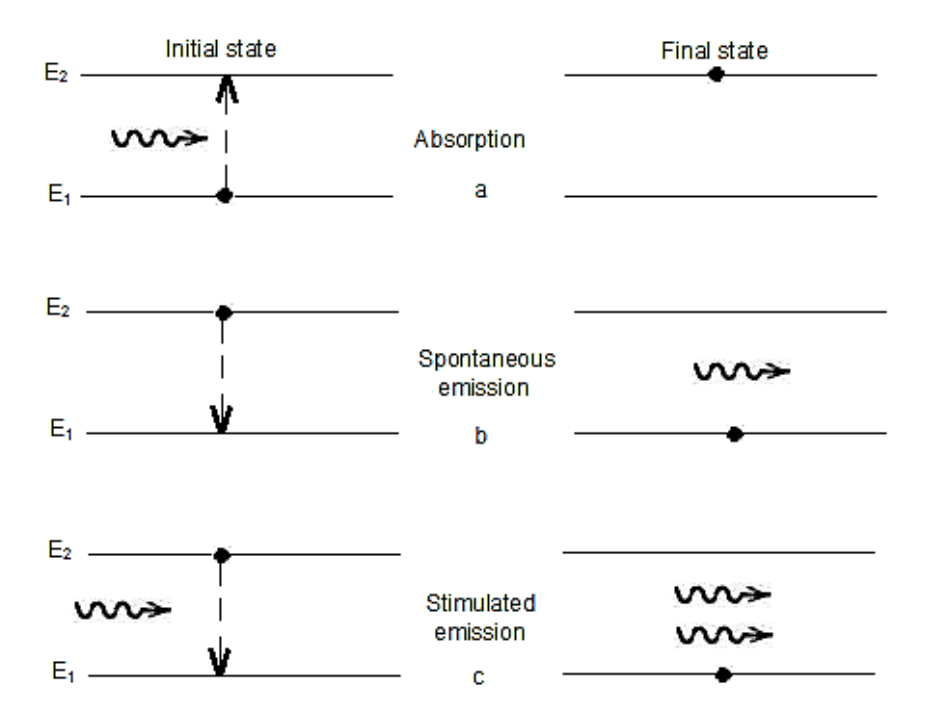


Figure 1.3 – Energy state diagram of fundamental processes.

2.2.2 Recombination Processes

In this section the recombination processes based on example of semiconductor laser are shown.

The recombination process of semiconductor material is associated with p-n junction, where n-type has majority free electrons and p-type has majority free holes. These two layers are separated by bandgap [3]. As a result, recombination of electron and holes can be radiative and non-radiative [1].

In a radiative recombination process the energy may release as light, however radiative recombination depends on many factors such as a semiconductor crystal condition and material, quantity of impurities, laser's bandgap type and laser structures overall [1]. Therefore, a non-radiative radiation can take place as well, which is undesirable as it decreases radiation of light. Among them are Auger recombination, surface and impurity recombination. For example, energy during the Auger recombination is emitted as a kinetic energy rather than light [2].

In order to evaluate above processes, the internal quantum efficiency can be defined as [2]:

$$\eta_{\rm int} = \frac{\tau_{nr}}{\tau_{rr} + \tau_{nr}},\tag{1.5}$$

where τ_{nr} and τ_{rr} - non-radiative and radiative recombination times respectively associated with the carriers. The index of internal quantum efficiency depends on semiconductor material and bandgap type.

Moreover, the parameter carrier lifetime τ_c , which shows the total recombination time of charged carriers without stimulated emission can be expressed as [2]:

$$1/\tau_c = 1/\tau_{rr} + 1/\tau_{nr} \tag{1.6}$$

Such indicators as Auger recombination and carrier density influence the value of carrier lifetime and can be determined as [2]:

$$1/\tau_{c} = A_{nr} + BN + CN^{2}, (1.7)$$

where Anr - non-radiative coefficient;

B - spontaneous radiative recombination coefficient;

C - Auger coefficient.

2.2.3 Population Inversion and Optical Gain

The population inversion process is described based on figure 1.4 [1].

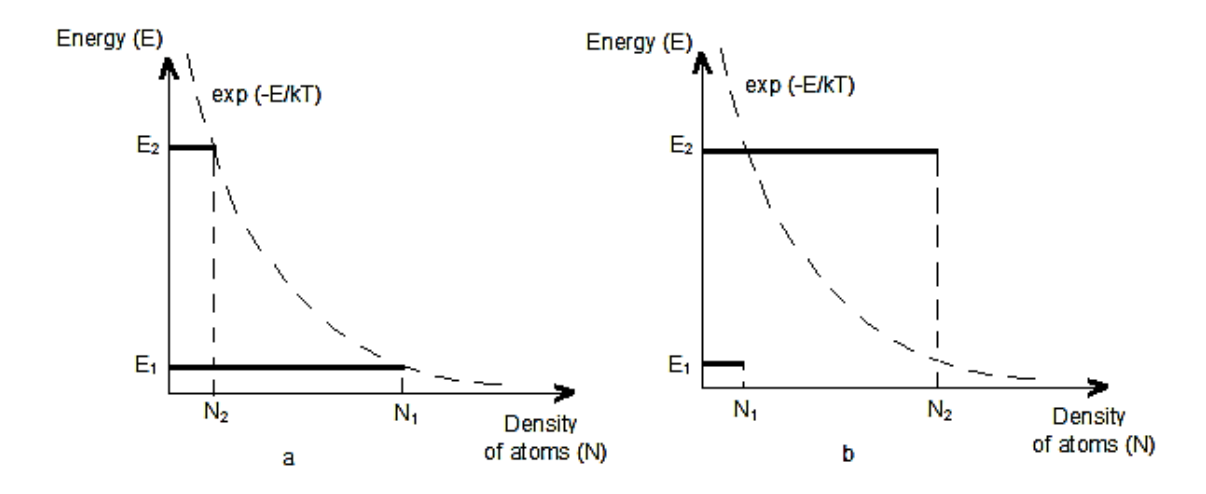


Figure 1.4 – Populations in a two energy level systems.

The figure (fig. 1.4 a) shows the Boltzmann distribution under the thermal equilibrium, where lower energy level E_1 has more atoms than upper energy level E_2 . However, optical amplification can be obtained in other case, when energy level E_2 has more atoms than the lower level. In other words, it is a nonequilibrium distribution of atoms, which shows a population inversion process (fig. 1.4 b). Usually, population inversion process is obtained by input of external energy source (by 'pumping') [1].

Further, explanation of population inversion and optical gain is given by using a common semiconductor laser structure, which consists of an active layer sandwiched between p-and n-type cladding layers (fig. 1.5) [19].

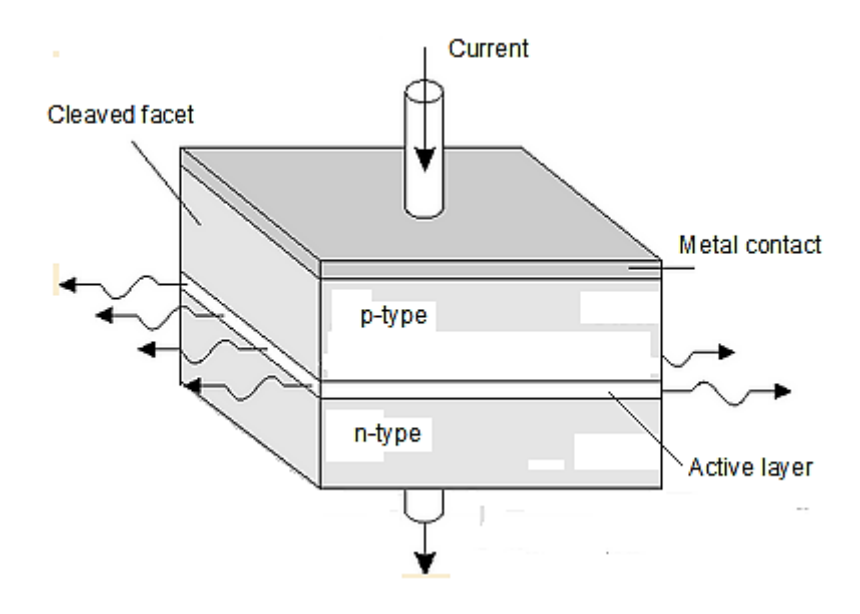


Figure 1.5 – Schematic of semiconductor laser structure.

Pumping in a semiconductor laser occurs electrically in a p-n junction. Population inversion happens when injected carrier density reaches a certain threshold, then optical gain produces in an active region. As a result, injected signal amplifies in the active region [2]. However, for laser oscillation condition the gain should be in balance with the total losses. Moreover, lasing requires an optical feedback as well which can be provided by cleaved facets. Other more detailed aspect of lasing condition and laser theory is outside of the project scope, however it can be found in the [1].

3 Methodology

3.1 Equivalent circuit of semiconductor laser based on lumped elements

The microwave optoelectronic laser model presented below (fig. 3.1) by Wong and Ghafouri-Shiraz [3] adapted from the research paper [4]. The initial model has been improved by matching signal source and intrinsic laser, which is necessary to avoid reflections as much as possible, as a result increasing a power output. Secondly, the actual circuit represents itself as an integrated model because the previous combined design involves laser equivalent circuit model and time domain model for simulating electrical parasitics and optical characteristics respectively. Lastly, the model considers different laser processes which were not included in the previous simplified model.

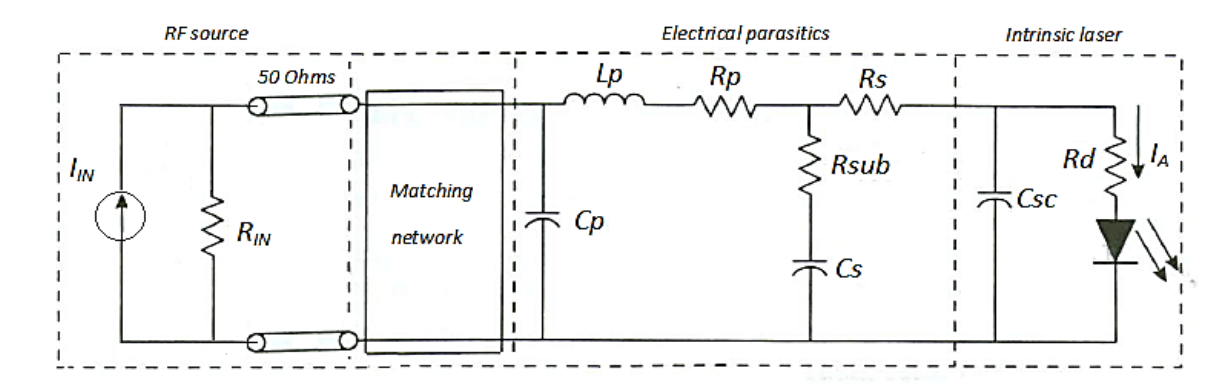


Figure 3.1 - Equivalent circuit of semiconductor laser.

The model depicted in Figure 3.1 comprises the following parts: RF source, matching network, electrical parasitics and intrinsic laser. The values of the equivalent circuit, which will be used in simulation, are given in table 3.1 from the source [20].

1 able 3.1 –	Paramete	ers of the	equiva	lent	circuit
--------------	----------	------------	--------	------	---------

Parasitic element	Value
Bondwire resistance, Rp	1.0 ohm
Bondwire inductance, Lp	0.63 nH
Stand-off shunt capacitance, C	0.23 pF
Chip substrate resistance, Rsub	1.5 ohms
Shunt parasitic capacitance, C	8.0 pF
Chip series resistance, Rs	5.5 ohms
Space-charge capacitance, C	2.0 pF
Forward bias resistance, RLD	2.0 ohms
Generator resistance, Rin	50 ohms

For more detailed explanation of the parts of laser it is required to refer to the original paper [20], where the structure and description of InGaAsP ridge waveguide are given (fig. 3.2) [3].

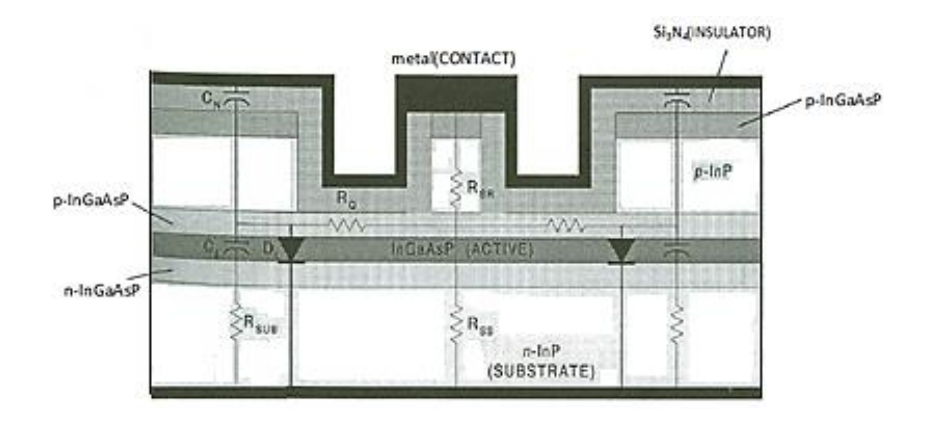


Figure 3.2 - The schematic cross section of the ridge waveguide laser.

3.1.1 RF source

Laser is feed from the source I_{IN} with a source resistance R_{IN} , transmission lines with characteristic impedance 50 Ohms are required for feeding the RF signal into the matching network part [3].

3.1.2 Intrinsic laser

Equivalent circuit of intrinsic laser is represented by laser diode and RC circuit of forward bias resistance R_d and space-charge capacitance C_{SC} [21]. The space-charge capacitance C_{SC} associated with the p-n junction of laser is formed between InGaAsP layers adjacent to the active layer (see element C_L at fig. 3.2) [20]. The junction resistance R_d is a carrier dependent and can be modelled by equation [3]:

$$Rd = \frac{2 \cdot k \cdot T}{q} \cdot \frac{\Delta t}{q \cdot v_a \cdot (N_{avg} - N_i)} \ln(\frac{N_{avg}}{N_i} + 1), \qquad (3.1)$$

where *k* - Boltzmann constant;

T - absolute temperature;

q - electronic charge;

 Δt - time step;

 v_a - active region volume;

 N_{avg} _average carrier density in the laser cavity;

N_i - intrinsic carrier density;

It should be noted that in a case when carrier is below threshold, the equivalent circuit described above is applicable. However, in a case when carrier is above the threshold value the RLC circuit is more suitable [21]. In this thesis it is assumed that constant value of R_d in both cases will be used for better computational efficiency [3].

3.1.3 Electrical parasitics

The Principle of operation of the laser without signal dispersion and any other losses occurring inside the laser can be assumed only in the ideal situation, which is unfortunately almost impossible to achieve in practice. According to a large number of studies [22,23,24 etc.] the presence of electrical parasitics significantly affects the laser performance, especially the small signal modulation. It is the cause of a roll-off in a modulation response and limitation of modulation bandwidth [25]. Taking into account these facts, the electrical parasitics should be included in the model to produce the simulation results close to to real laser performance.

In fact, electrical parasitics (unwanted inductance, capacitance, resistance) are related with the laser structure and described in detail below.

The chip series resistance R_S in series with active region and shunt parasitic capacitance C_S between the metal contact are prevailing electrical parasitics throughout the laser structure. The chip series resistance is a result of ridge resistance (see R_{SR} in fig.3.2) associated with metal-active layer contact and resistance associated with substrate under the active region (see R_{SS} in fig.3.2). The shunt parasitic capacitance is related with capacitance of a silicon nitride insulator layer (see C_N in fig.3.2) in series with space-charge capacitance (see C_L in fig.3.2). Another parasitics associated with a bondwire are: bondwire resistance R_p , bondwire inductance L_p and stand-off shunt capacitance C_p [20].

3.1.4 Matching network

The proposed integrated model shown above is also considered a matching network part. Generally, matching network is intended to increase power output by minimizing losses due to impedance mismatch. Moreover, it may also improve the signal-to-noise ratio of the system [26].

The choice of the matching network may be based on the following aspects [26]:

- Complexity. The less complicated design is dominant among other, because of cheap cost, small size and high reliability. Although, it is necessary to take into account tradeoff between design and the purpose;
- Bandwidth. Matching circuit for a single frequency can perform its function ideally, however matching for a broadband operation requires more complex configuration of matching circuit;
- Implementation. A particular model of matching network sometimes is suitable for specific waveguide;
- Adjustability. Several model of matching network can consider the tunable load impedance, which is required for several devices.

Following the same reasons, in order to improve power transfer between the signal source and laser diode simplest method of linking a chip resistor (43-48 Ohms) in series with the laser diode can be chosen. However, for obtaining a broad bandwidth pseudo-bandpass LC ladder network or resonant circuit step transformer can be useful. For the narrow bandwidth the quarter-wave transformer or stub tuning can be applied [3].

Moreover, matching network can be designed by lumped or distributed elements. Distributed elements have a big size at lower microwave frequencies [27]. However, at frequencies greater than 1 GHz lumped elements are difficult to realize [3]. Therefore, monolithic integration of Metal-Insulator-Metal (MIM) capacitor and inductor of a microwave reactive matching networks will be used here. This technique presented by Maricot et.al. [28] allows minimizing effect of electrical parasitics on the matching network at higher frequency operation.

With reference to the above, the simplest L-section type of matching network is chosen. Two configurations for operation below and at 6.6GHz are shown in figure 3.3 a, b [26] respectively. The reactive elements jX and jB can be either inductors or capacitors considering the load impedance.

Therefore, at first step the load impedance (resulting impedance of the parasitics network) for the 2 cases is defined as (Appendix A):

$$Z_{1} = R_{sub} + 1/(i \cdot 2 \cdot \pi \cdot f \cdot C_{S});$$

$$Z_{2} = (R_{S} \cdot Z_{1})/(R_{S} + Z_{1});$$

$$Z_{3} = R_{p} + (i \cdot 2 \cdot \pi \cdot f \cdot L_{p});$$

$$Z_{4} = Z_{2} + Z_{3};$$

$$Z_{5} = 1/(i \cdot 2 \cdot \pi \cdot f \cdot C_{p});$$

$$Z_{L} = (Z_{4} \cdot Z_{5})/(Z_{4} + Z_{5})$$
(3.2)

By changing the matching frequency, the load impedance is equal:

- for frequency 1.1 GHz $Z_L=0.1198 + 0.0571i$;
- for frequency 6.6 GHz $Z_L = 0.0972 + 0.6379i$.

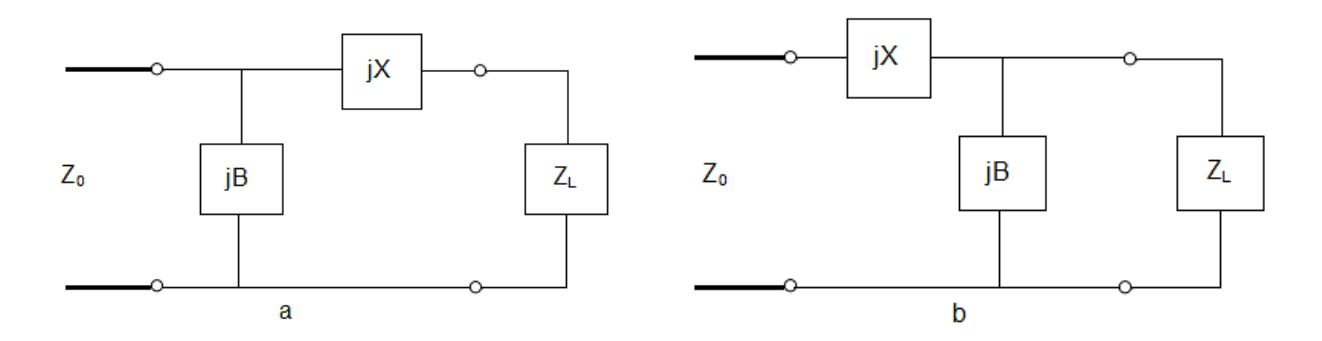


Figure 3.3 – L-section matching network.

At the second step, it is necessary to find the values of the reactive elements. For this purpose analytic solution is used [26].

For frequency 1.1 GHz (Fig. 3.3 a):

The impedance-matched condition is given as [26]:

$$\frac{1}{Z_0} = jB + \frac{1}{R_L + j(X + X_L)} \tag{3.3}$$

By using simple mathematical transformation the values of reactive elements can be calculated [26]:

$$B \cdot Z_0 \cdot (X + X_L) = Z_0 - R_L$$

 $(X + X_L) = B \cdot Z_0 \cdot R_L$

$$X = \pm \sqrt{R_L \cdot (Z_0 - R_L)} - X_L \tag{3.4}$$

$$B = \pm \frac{\sqrt{(Z_0 - R_L)/R_L}}{Z_0} \tag{3.5}$$

$$C = -\frac{1}{2 \cdot \pi \cdot f \cdot X} \tag{3.6}$$

$$L = -\frac{1}{2 \cdot \pi \cdot f \cdot B} \tag{3.7}$$

For frequency 6.6 GHz (Fig. 3.3 b):

The impedance-matched condition is given as [26]:

$$Z_0 = jX + \frac{1}{jB + 1/(R_L + jX_L)}$$
(3.8)

By using simple mathematical transformation the values of reactive elements can be calculated [26]:

$$B(X \cdot R_L - X_L \cdot Z_0) = R_L - Z_0$$

$$X(1 - B \cdot X_L) = B \cdot Z_0 \cdot R_L - X_L$$

$$B = \frac{X_L \pm \sqrt{R_L / Z_0} \cdot \sqrt{R_L^2 + X_L^2 - Z_0 \cdot R_L}}{R_L^2 + X_L^2}$$
(3.9)

$$X = \frac{1}{B} + \frac{X_L \cdot Z_0}{R_L} - \frac{Z_0}{B \cdot R_L}$$
 (3.10)

$$C = \frac{B}{2 \cdot \pi \cdot f} \tag{3.11}$$

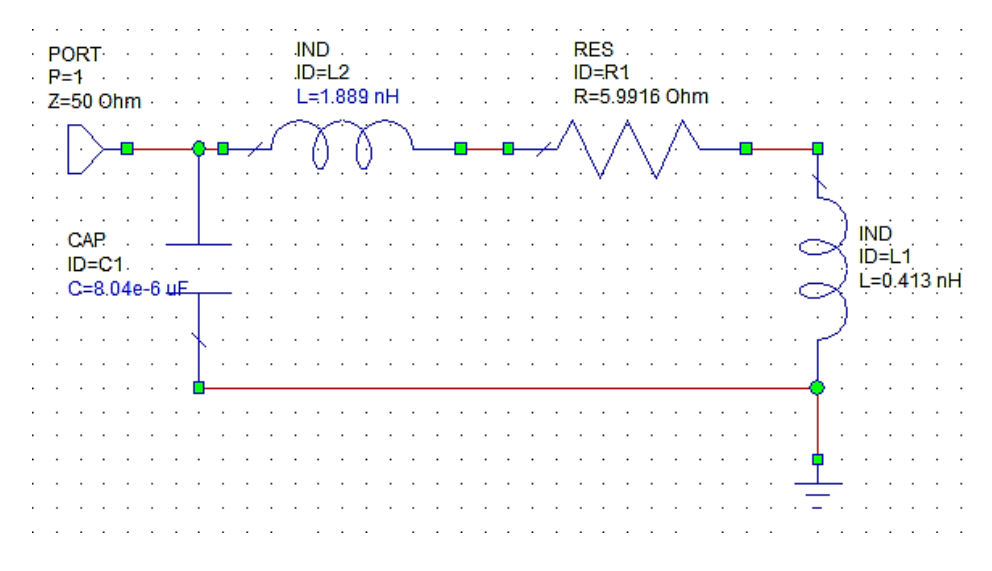
$$L = -\frac{X}{2 \cdot \pi \cdot f} \tag{3.12}$$

With reference to the above, the calculated value of the capacitor and inductor are shown in the table 3.2 (matlab code is shown in Appendix A).

Table 3.2 – The values of the reactive elements of the L-section matching network

Nth subharmonic frequency	Lmatch (nH)	Cmatch(pF)
6 th (1.1 GHz)	2.6693	7.5774
5 th (1.32 GHz)	2.2244	6.3145
4 th (1.65 GHz)	1.7795	5.0516
3 rd (2.2 GHz)	1.3347	3.7887
2 nd (3.3 GHz)	0.8898	2.5258
Fundamental (6.6GHz)	2.1583	0.9558

Moreover, in order to obtain the better results, tuning the values of the reactive elements can be implemented in AWR microwave office environment. The following circuits in the figure 3.4 are designed for frequency 6.6GHz (b) and below (a). The circuits contain a load impedance part, which is represented by resistor and inductor (due to the reactive part of the load impedance at both cases are positive values) and L-section matching part as well. By setting the L and C elements as a variable, the lowest return loss parameter S11 (figure 3.4) can be achieved [29]



а

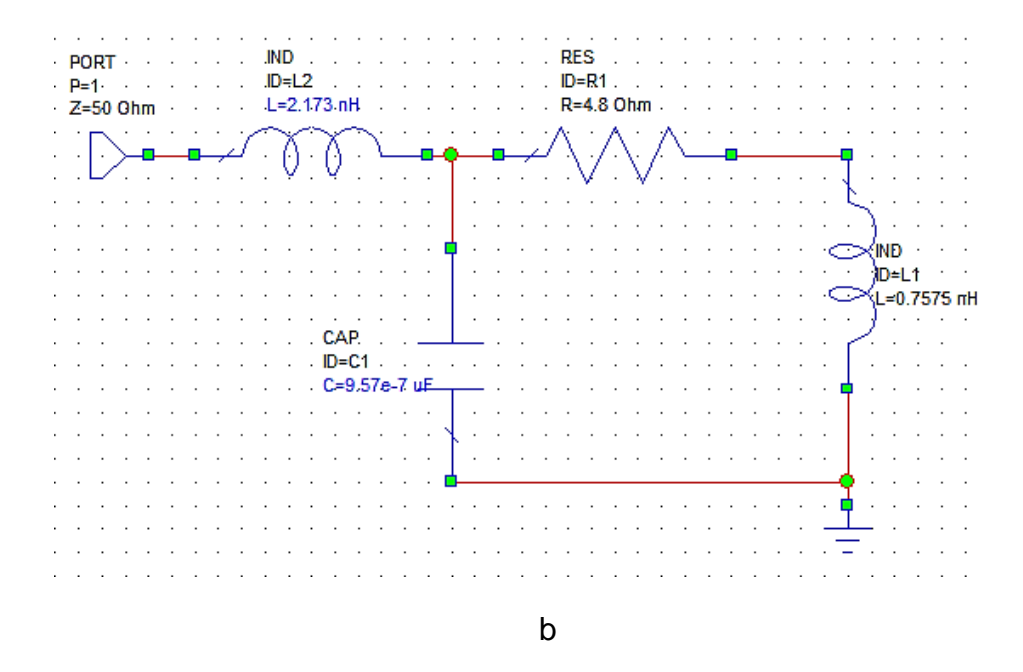


Figure 3.4 - L-section matching network for frequencies below (a) and at (a) 6.6 GHz implemented in AWR microwave office.

By conducting several experiments it has been identified that lowest value of insertion loss (S11= - 35dB) is achieved when C=1.889nH and L=8.04pF for the 1.1GHz, and S11= - 40dB when C=2.173nH and L=0.957pF for 6.6 GHz.

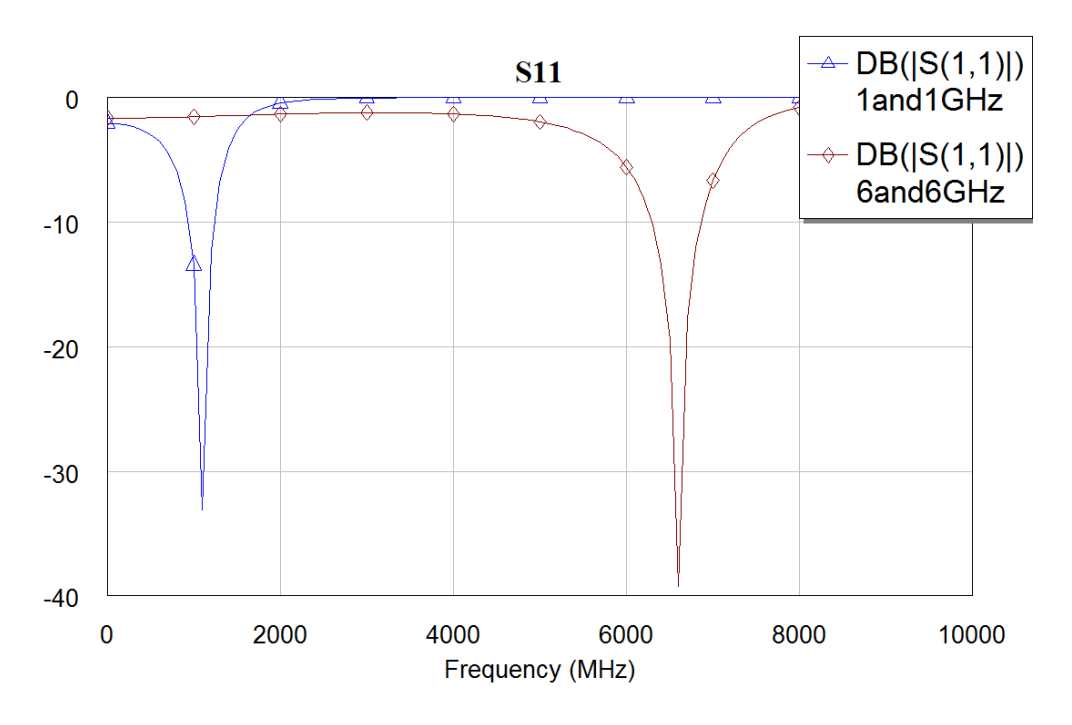


Figure 3.5 - Return loss (S11 parameter).

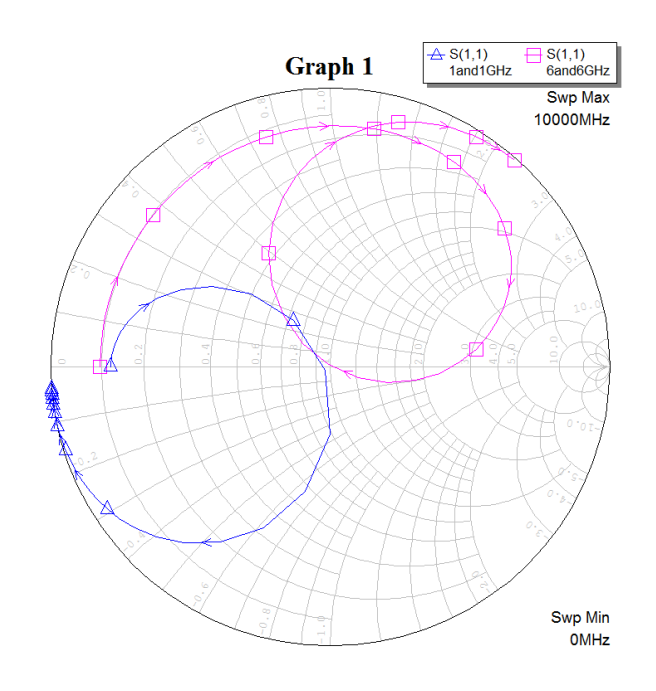


Figure 3.6 - Smith chart.

Finally, the latest version of the L-section matching networks are depicted in figure 3.7 for 6.6GHz (b) and below frequencies (a) respectively.

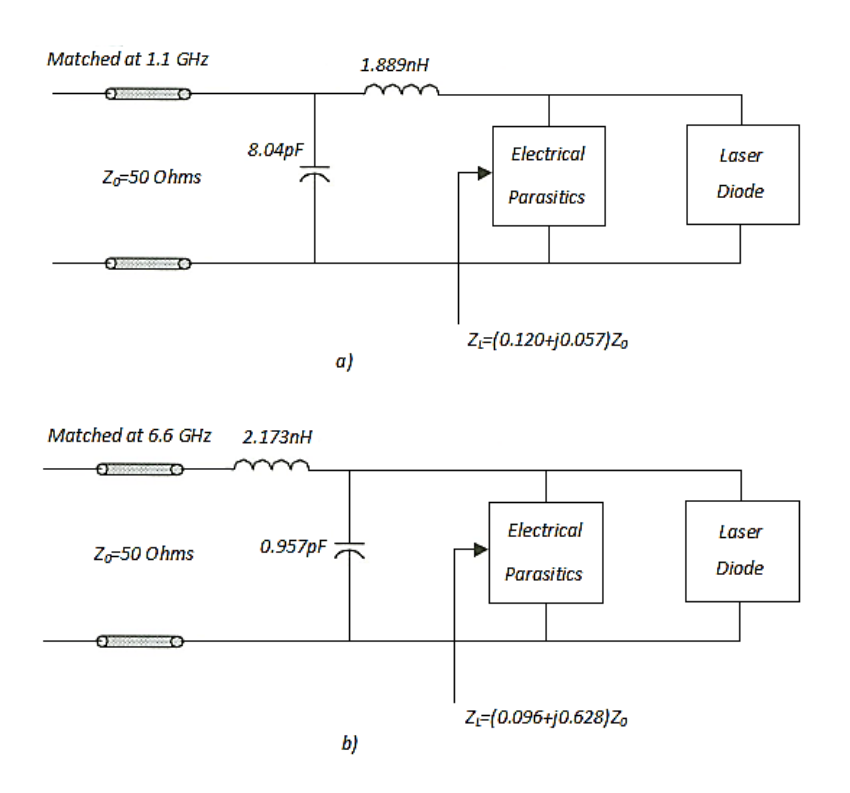


Figure 3.7 - Matching network.

Since all parts of the model have been discussed in detail, further the TLLM technique will be applied for the whole integrated model.

3.2 The TLLM algorithm

The laser modelling approach by using Transmission-Line Laser Model has been given in detail in suitable publications by Lowery [17,30,31,32]. According to that theory, TLLM represents a laser cavity as a number of equal sections in conditions of discrete space and time. Each section contains a scattering node, which represents optical processes as stimulation emission, spontaneous emission, and attenuation. The connection between the adjacent sections is performed by transmission lines, considering the wave propagation delay. These basic processes of scattering and connection form a TLLM algorithm [9]. Implementation of TLLM algorithm allows representing all physical processes occurring in the model as a special customer written program for laser simulation in a computer [33]. In this thesis Matlab software will be used for time-domain laser simulation.

Simulation of this model is performed in a time-domain. The process starts when input pulse incident to the first section. That incident voltage pulse automatically scatters by applying scattering matrix. Then, the generated reflected pulse of the first node becomes incident to the adjacent node by travelling through the link transmission line. As a result, this process repeats each iteration by propagating pulse further in next adjacent node and so on [33]. Thus voltage propagation process represents an optical field of the laser cavity [34].

Moreover, the carrier density in each section is defined during the operation by solving the carrier rate equation. Hence, local alteration of carrier density impacts the optical gain, which in turn regulates the scattering and connecting algorithm at the next iteration [33]. The laser facets are represented by unmatched terminations [3].

With reference to the above, instantaneous optical power by collecting output pulse in a time domain and output spectrum by applying a Fast Fourier Transform (FFT) can be obtained [34, 35].

3.3 The TLLM method of physical parameters of the laser

3.3.1 TLM link and stub modelling

In order to implement TLLM, it is necessary to represent lumped elements of the integrated model by a transmission lines in a discrete form. This allows simulating model in a time domain as a transmission line represents itself as a wave propagation medium.

Therefore, reactive lumped elements can be replaced by TLM link-lines (fig.3.8) and TLM stub-lines (fig.3.9) [3].

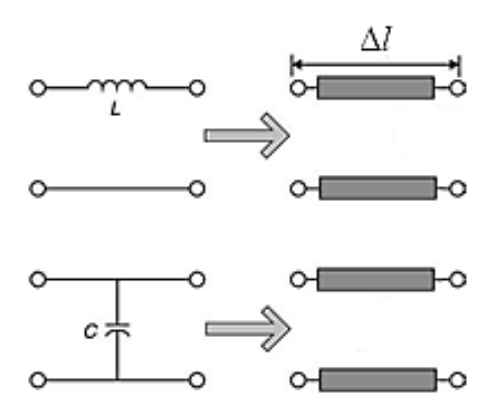


Figure 3.8 – TLM link-lines.

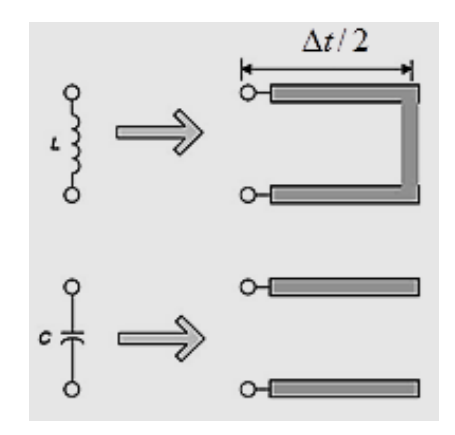


Figure 3.9 – TLM stub-lines.

This modelling approach is discussed in detail in the research paper by Bandler et.al. [36]. General modelling aspects are presented below.

First of all, it is assumed that length of the all transmission line models have the same value and propagation time through the line (Δt) as well.

In order to the link modelling the velocity of propagation in a case of lossless transmission line is defined as [3]:

$$v_p = \frac{1}{\sqrt{L_d \cdot C_d}} = \frac{\Delta l}{\Delta t} \tag{3.13}$$

where Ld - inductance per unit length;

Cd - capacitance per unit length;

 Δl - unit section length;

 Δt - the model timestep.

The lumped inductor can be expressed as:
$$L = \Delta l \cdot Ld$$
; (3.14)

From the formula 3.13 the capacitance per unit length can be defines as:

$$Cd = \left(\frac{\Delta t}{\Delta l}\right)^2 \cdot \frac{1}{Ld} \tag{3.15}$$

The characteristic impedance of the line shows scattering behavior of the pulse and by using formulas 3.14, 3.15 is presented as:

$$Z_0 = \sqrt{\frac{Ld}{Cd}} = \frac{L}{\Delta t} \tag{3.16}$$

Consequently, repeating the above steps, the characteristic impedance for capacitor can be easily found:

$$Z_0 = \frac{\Delta t}{C} \tag{3.17}$$

For the stub line, propagation time to the end of stub and back is equal Δt , therefore impedance for the inductor and capacitor can be defined as:

$$Z_0 = \frac{2 \cdot L}{\Delta t} \tag{3.18}$$

$$Z_0 = \frac{\Delta t}{2 \cdot C} \tag{3.19}$$

It is important to note that approximation error occurring in the models can be avoided by choosing the small value of Δt .

3.3.2 The laser-transmitter model based on TLLM

After the introduction of modelling principles, the integrated laser model (fig. 3.1) can be replaced by equivalent model based on TLLM (fig.3.10).

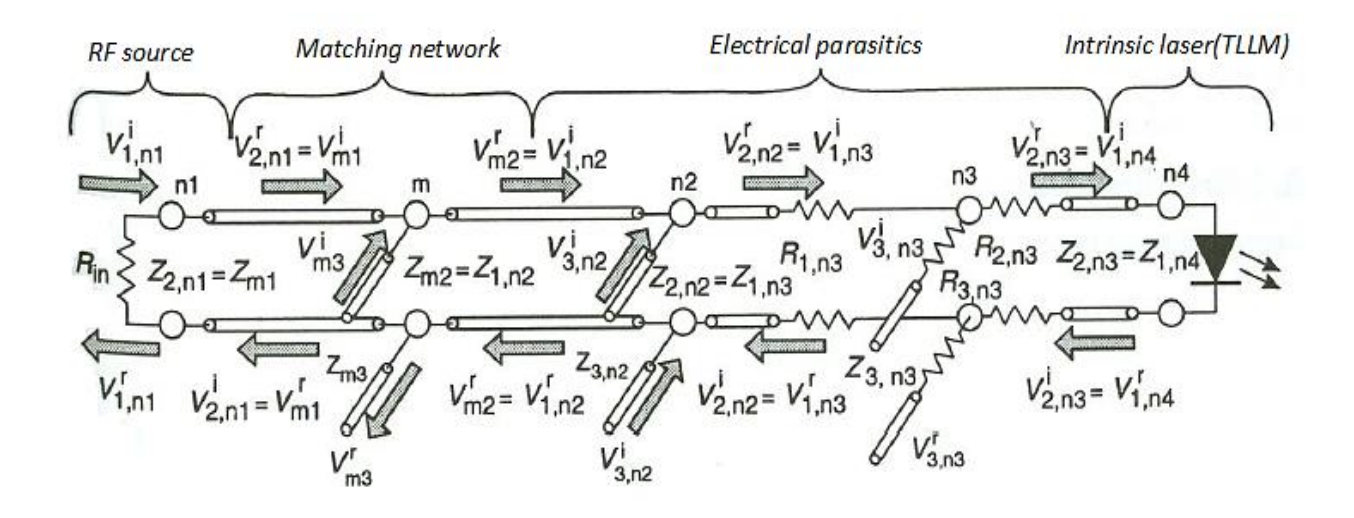


Figure 3.10 - The equivalent of laser-transmitter model based on TLLM.

The model consist of TLM lines, scattering nodes, active resistors and laser diode.

The TLM link-lines are equivalent to the lumped bondwire inductance and lumped spacecharge capacitance with impedances:

$$Z_{LP} = \frac{L_p}{\Lambda T} \tag{3.20}$$

$$Z_{CSC} = \frac{\Delta T}{C_{SC}} \tag{3.21}$$

And TLM stub-lines are equivalent of the lumped stand-off shunt capacitance and lumped shunt parasitic capacitance as well:

$$Z_{CP} = \frac{\Delta T}{2 \cdot C_P} \tag{3.22}$$

$$Z_{CS} = \frac{\Delta T}{2 \cdot C_{S}} \tag{3.23}$$

The representing of lumped elements by TLM lines in the matching network part depends on matching frequency as mentioned before:

- matched at frequencies below 6.6 GHz:

 $Z_{m1} = 50 \, Ohms$ is a 'transmission line feeding the RF signal into the matching circuit' [3].

The inductance and capacitance of matching part are modelled by TLM link-lines and TLM stub-lines respectively:

$$Z_{m2} = \frac{L_{match}}{\Delta t} \tag{3.24}$$

$$Z_{m3} = \frac{\Delta t}{2 \cdot C_{match}} \tag{3.25}$$

- matched at frequency 6.6 GHz:

In the second type of matching network, the inductance changes the position as shown in Figure 3.7b, therefore feeding transmission line is not necessary here:

$$Z_{m1} = \frac{L_{match}}{\Delta t} \tag{3.26}$$

Moreover, in order to model link-line between the node m and n2 it is required to divide proportionally the stand-off shunt capacitance to the link-line and stub-line. Hence, the characteristic impedances are equal:

$$Z_{m2} = \frac{\Delta t}{C_n / 2} \tag{3.27}$$

$$Z_{m3} = \frac{\Delta t}{2 \cdot C_p / 2} \to \frac{\Delta t}{C_p} \tag{3.28}$$

The principle of scattering and connecting algorithm will be described in the next section.

3.3.3 Scattering and connecting process

As discussed before the scattering and connecting algorithm of the TLLM can be represented by a matrix. Therefore the relations between the incident and reflected pulse are shown as follows [3]:

$$_{k}V^{rT} = S_{k} \cdot V^{iT}$$
 [scattering] (3.29)

$$_{k+1}V^{iT} = C_k \cdot V^{rT}$$
 [connecting] (3.30)

where V^{iT} , V^{rT} - transpose matrix considering incident and reflected pulses of each branches of the node;

k, k+1 - k or k+1 time iteration;

 S_k , C_k - scattering and connecting matrices.

More detailed explanation is given based on figure 3.10. The scattering nodes are described as n1, m, n2, n3, n4. For instance, the input pulse V_1^i incident to a node n1, then this pulse V_1^i scatters by using scattering matrix (eq. 3.32). Resulting reflected pulse V_2^r , n1 from the node n1 is defined from the equation 3.31. Moreover, this reflected pulse becomes incident to the node m through a common branch (TLM link-line) therefore V_2^r , $n1 = V^i m1$. Although, the connecting process can be described by matrix, in this thesis for better computational efficiency the way shown before is chosen. Further, scattering process for node m, n2, n3 is expressed as equation 3.33, where for the nodes m, n2 the value of R_{mi} should be set to the zero, due to this nodes consider lossless TLM lines. Finally, the pulse propagation reaches the last node n4, which describes the process by matrix in equation 3.35.

It is important to note, that in an unmatched case the total number of nodes is reduced by one node m, therefore V_2^r , $n1 = V_1^i$, n2.

The scattering matrix for input node (n1), having 2 branches is expressed as:

$$\begin{bmatrix} V_1^r, n1 \\ V_2^r, n1 \end{bmatrix} = Sk_1 \cdot \begin{bmatrix} V_1^i, n1 \\ V_2^i, n1 \end{bmatrix}, \tag{3.31}$$

where
$$Sk_1 = \begin{bmatrix} \frac{Zm1 - Rin}{Rin + Zm1} & \frac{2 \cdot Rin}{Rin + Zm1} \\ \frac{2 \cdot Zm1}{Rin + Zm1} & \frac{Rin - Zm1}{Rin + Zm1} \end{bmatrix}$$
 (3.32)

The scattering matrix for nodes (m, n2, n3), having 3 branches is expressed as:

$$\begin{bmatrix} V_{m1}^r \\ V_{m2}^r \\ V_{m3}^r \end{bmatrix} = C_m \cdot Sk(m, n2, n3) \cdot \begin{bmatrix} V_{m1}^i \\ V_{m2}^i \\ V_{m3}^i \end{bmatrix}$$
(3.33)

$$Sk(m, n2, n3) = \begin{bmatrix} 2 \cdot P_{m1} \cdot Z_{s2} \cdot Z_{s3} + R_{m11} & 2 \cdot P_{m1} \cdot Z_{s1} \cdot Z_{s3} & 2 \cdot P_{m1} \cdot Z_{s1} \cdot Z_{s2} \\ 2 \cdot P_{m2} \cdot Z_{s2} \cdot Z_{s3} & 2 \cdot P_{m2} \cdot Z_{s1} \cdot Z_{s3} + R_{m22} & 2 \cdot P_{m2} \cdot Z_{s1} \cdot Z_{s2} \\ 2 \cdot P_{m3} \cdot Z_{s2} \cdot Z_{s3} & 2 \cdot P_{m3} \cdot Z_{s1} \cdot Z_{s3} & 2 \cdot P_{m3} \cdot Z_{s1} \cdot Z_{s2} + R_{m33} \end{bmatrix}$$
(3.34)

where for i=1,2,3

$$C_{m} = \frac{1}{Z_{s1} \cdot Z_{s2} + Z_{s1} \cdot Z_{s3} + Z_{s2} \cdot Z_{s3}}$$

$$R_{mii} = \frac{R_{mi} - Z_{mi}}{R_{mi} + Z_{mi}}$$

$$Z_{si} = R_{mi} + Z_{mi}$$

$$P_{mi} = \frac{Z_{mi}}{R_{mi} + Z_{mi}}$$

$$Sk(n4) = \begin{bmatrix} \frac{Rld - Z_{1,n4}}{Rld + Z_{1,n4}} & \frac{2 \cdot Z_{1,n4}}{Rld + Z_{1,n4}} \\ \frac{2 \cdot Rld}{Rld + Z_{1,n4}} & \frac{Z_{1,n4} - Rld}{Z_{1,n4} + Rld} \end{bmatrix}$$
(3.35)

3.4 The TLLM method of optical processes inside the laser-transmitter

Optical processes mentioned in a Background section play an important role of laser performance and hence they are also taken into account in the model. The figure 3.11 visually presents how TLLM implements all optical processes. Information about local carrier density (N_n) and local photon density (S_n) inside the laser section is modelled by using rate equations, which describe transition of energy between electrons and photons through absorption, spontaneous and stimulated emission. Meanwhile the optical gain and spontaneous emission noise are considered by scattering matrix [3].

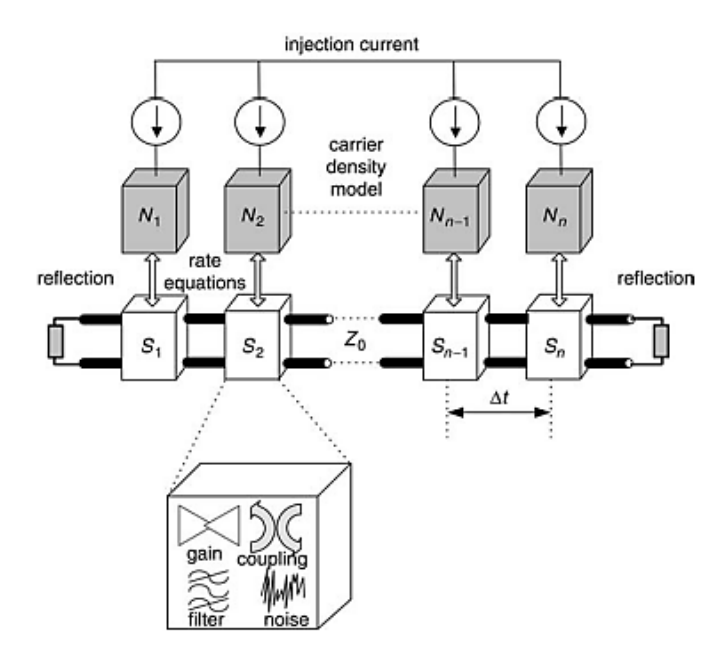


Figure 3.11 – The TLLM considering optical process.

3.4.1 Carrier density model

In order to describe the carrier density model the carrier rate equation is used and expressed as follows [3]:

$$\frac{dN}{dt} = \frac{I}{q \cdot v_a} - \frac{N}{\tau_n} - G(N) \cdot S \tag{3.36}$$

where N - carrier density;

I - injected current;

 v_a - active layer volume;

q - electronic charge;

 τ_n - carrier lifetime;

G(N) - stimulated recombination rate;

S - photon density.

Furthermore, the carrier rate equation can be modelled as an equivalent circuit (fig. 3.12) and described by its analogue equation 3.37 [3].

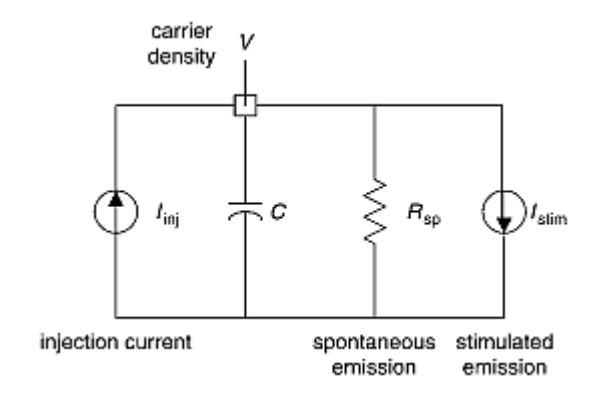


Figure 3.12 – The equivalent circuit of the carrier density rate equation.

$$\frac{dQ}{dt} = I_{inj} - \frac{V}{R_{sn}} - I_{stim} \tag{3.37}$$

where $Q = N \cdot q \cdot v_a = C \cdot V$;

 I_{ini} -injected current into active region;

C - storage capacitor describes carrier build-up;

 R_{sp} - resistor describes a spontaneous emission rate;

 $I_{\mbox{\tiny stim}}$ - stimulated emission rate.

To sum up and comparing above, the following system of equations will be used in simulation [3]:

$$\begin{cases} I_{inj} = I \\ R_{sp} = \frac{\tau_n}{q \cdot v_a} \\ I_{stim} = q \cdot v_a \cdot G(N) \cdot S \end{cases}$$
 (3.38)

Regarding the photon density, it can be defined as [3]:

$$S_{n} = \frac{n_{g} \cdot (\left|F_{M}^{i}(n)\right|^{2} + \left|B_{M}^{i}(n)\right|^{2})}{Z_{p} \cdot h \cdot f_{0} \cdot c_{0} \cdot m^{2}}$$
(3.39)

where $n_{\rm g}$ - effective group index;

h - Planck's constant;

 f_0 - lasing frequency;

 c_0 - speed of light;

 Z_p - wave impedance;

m - unity constant with dimension of length;

 $F_{\it M}^{\it i}(n)$ - forward voltage pulse on the main transmission-line of n section;

 $B_{M}^{i}\left(n\right)$ - backward voltage pulse on the main transmission-line of n section;

3.4.2 Amplification Model

As in a previous case, modelling laser gain spectrum follows the same principle involving the block diagram (Fig.3.13) and corresponding equation (eq.3.40) [3].

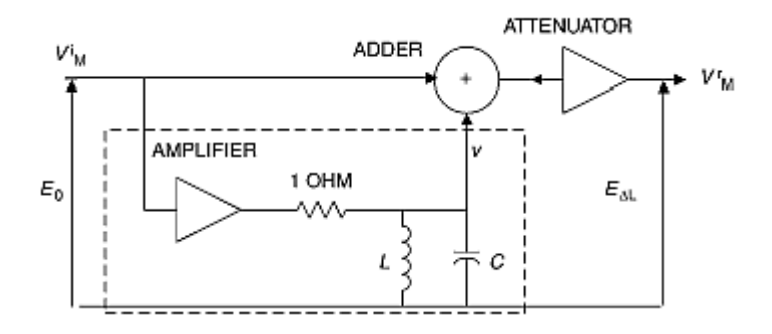


Figure 3.13 – Block diagram of the gain filter.

In figure 3.13 the RLC bandpass filter represents a small amplified signal $\left(\frac{\Delta L \cdot \Gamma \cdot g}{2}\right) \cdot E_0$, which is added with an incoming signal E_0 and attenuated by factor $\exp\left(-\frac{\alpha_{sc} \cdot \Delta L}{2}\right)$. As a result the output signal from the diagram is an amplified signal $E\Delta L$ [3].

$$E_{n\Delta L} = E_{(n-1)\Delta L} \left(1 + \frac{\Delta L \cdot \Gamma \cdot g}{2} \right) \exp\left(-\frac{\alpha_{sc} \cdot \Delta L}{2} \right)$$
(3.40)

E - optical field amplitude;

 ΔL - propagating distance;

 Γ - confinement factor;

g - frequency - dependent gain coefficient;

 α_{sc} - loss factor;

The TLM representation of the stub filter model is shown in the figure 3.14 [3], where lumped inductance and capacitance are represented as short and open circuit of TLM stubs [3].

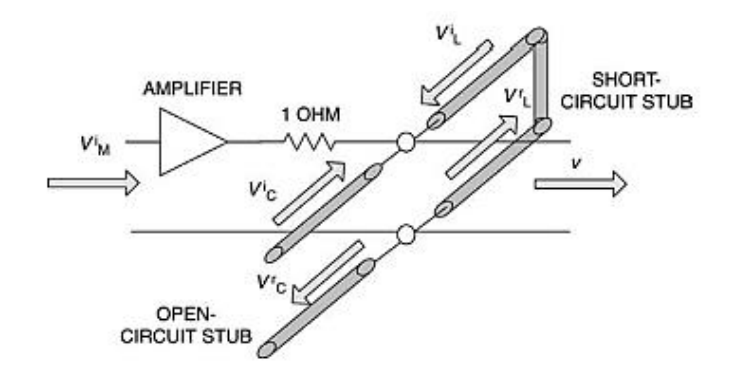


Figure 3.14 - The TLM stub filter.

The scattering matrix of this process is defined as follows [3]:

$$\begin{bmatrix} V_M \\ V_C \\ V_L \end{bmatrix}^r = \frac{1}{y} \cdot \begin{bmatrix} t(g+y) & 2 \cdot t \cdot Y_c & 2 \cdot t \cdot Y_L \\ g & 2 \cdot Y_c - y & 2 \cdot Y_L \\ g & 2 \cdot Y_c & 2 \cdot Y_L - y \end{bmatrix}_{k} \cdot \begin{bmatrix} V_M \\ V_C \\ V_L \end{bmatrix}^i$$
(3.41)

where V_{M} , $V_{C,}$, V_{L} - voltage pulses on the main transmission-line, inductive stub line and capacitive stub line as well;

$$y = 1 + Y_C + Y_L$$
;

$$t = \exp\left(-\frac{\alpha_{sc} \cdot \Delta L}{2}\right);$$

Depending on gain coefficient value, the model can be linear or logarithmic. In the thesis the linear model is assumed with a gain coefficient value less than 10⁻¹⁰ and is defined as [3]:

$$g = a \cdot v_g \cdot (N - N_{tr}) \frac{S}{(1 + \varepsilon) \cdot S}$$
(3.42)

where a - differential gain constant;

 $v_{\rm g} = c_{\rm 0} \, / \, n_{\rm g}$ - group velocity defined from speed of light $\, c_{\rm 0} \,$ and effective group index $\, n_{\rm g} \,$;

 ε - gain compression factor;

S - photon density in the local model;

N - average carrier density;

 $N_{\it th}$ - threshold carrier density.

The admittances of the inductive stub line and capacitive stub line are equal to equation 3.43. The more detailed derivation of this equation can be found in [3].

$$Y_L = Q \cdot \tan(\pi \cdot f_0 \cdot \Delta t) \text{ and } Y_C = \frac{Q}{\tan(\pi \cdot f_0 \cdot \Delta t)}$$
 (3.43)

where Q is a Q – factor, ratio of central frequency to its bandwidth.

The connection between the section for forward (F) and backward (B) travelling wave occurs by the following rules [3]:

$${}_{k+1}F_M^i(n) = {}_kF_M^r(n-1) \tag{3.44}$$

$$_{k+1}B_{M}^{i}(n)=_{k}B_{M}^{r}(n+1)$$

The connecting algorithm at the facets is described by equation 3.45, where pulse reflected from the facet changes travelling direction on the opposite side [3].

$${}_{k+1}F_M^i(1) = \sqrt{R_1} \cdot {}_k B_M^r(1) \tag{3.45}$$

$$_{k+1}B_{M}^{i}(S) = \sqrt{R_{2}}_{k}F_{M}^{r}(S)$$

- R_1 and R_2 are values of power reflectivity at the left and right facets.

Lastly, connection process for stubs is defined as [3]:

$${}_{k+1}V_C^i(n) = {}_kV_C^r(n)$$

$${}_{k+1}V_L^i(n) = -{}_kV_L^r(n)$$
(3.46)

3.4.3 Laser Chirp Modelling

The injection current accompanied by varying of carrier density can be the cause of refractive index change, which subsequently affects the lasing frequency by shifting it [38]. This dynamic shift is known as frequency or wavelength chirping. It directly relates with linewidth enhancement factor and can cause pulse spreading [3].

Modelling of this process can be achieved by stub - attenuator model (Figure 3.15), where phase (adjusting) stub regulates phase length, which in turn varies a refractive index change. This stubs are situated at the facets, however in order to consider inhomogeneous distribution of carrier density it is required to locate it in each section. In this thesis only the first case is assumed [3].

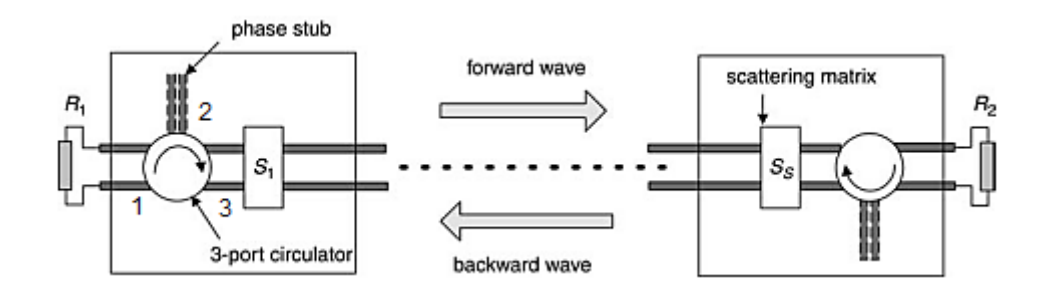


Figure 3.15 - Stub- attenuator model.

The principle of stub-attenuator operation is shown as follows. The reflected voltage pulses from the terminal (facet) input to the phase-stub. This phase-stub delays voltage propagation along the main transmission-line by three-port circulator. For instance, incident pulse from the left facet to the port 1 of the circulator goes to the port 2, reflected from the stub (produce a delay) and continues its propagation by exiting from port 3 to the main transmission line. This process is implemented in a scattering matrix [3]:

$$\begin{bmatrix} V_{1}(1) \\ V_{2}(1) \\ V_{3}(1) \end{bmatrix}^{r} = \begin{bmatrix} 0 & 0 & 1 \\ \frac{2 \cdot Z_{S}}{(1 + Z_{S})} & \frac{(1 - Z_{S})}{(1 + Z_{S})} & 0 \\ \frac{(Z_{S} - 1)}{(Z_{S} + 1)} & \frac{2}{(1 + Z_{S})} & 0 \end{bmatrix} \cdot \begin{bmatrix} V_{1}(1) \\ V_{2}(1) \\ V_{3}(1) \end{bmatrix}^{i}$$
(3.47)

where $Z_{\rm S}$ is the phase-stub impedance.

It is important to note that TLLM requires synchronization, therefore only value of the stub impedance can be changed. Despite this, there is relation between the stub impedance and stub length. In order to figure out this relation, it is necessary to equate the input impedances of the adjustable and fixed length stubs (eq. 3.48, 3.49). Moreover, it will be done by taking into account the carrier concentration level, which determines when open or short circuits stub is required [3].

1st case: Open circuit stub (capacitive stub).

In this case, negative variation of carrier concentration level (ΔN) leads to a positive change of phase length [3].

$$\frac{Z_0}{j \cdot \tan(\beta \cdot \Delta l_{ph})} = -j \cdot Z_S \cdot \cot(\pi \cdot f_0 \cdot \Delta t) \to Z_{S(C)} = \frac{Z_0 \cdot \tan(\pi \cdot f_0 \cdot \Delta t)}{\tan(\beta \cdot \Delta l_{ph})}$$
(3.48)

2nd case: Short circuit stub (inductive stub).

In this case, positive variation of carrier concentration level (ΔN) leads to a negative change of phase length [3].

$$\frac{Z_0}{j \cdot \tan(\beta \cdot \Delta l_{ph})} = j \cdot Z_S \cdot \tan(\pi \cdot f_0 \cdot \Delta t) \to Z_{S(L)} = \frac{Z_0}{\tan(\pi \cdot f_0 \cdot \Delta t) \cdot \tan(\beta \cdot \Delta l_{ph})}$$
(3.49)

where phase length is equal
$$\Delta l_{ph} = \frac{\Gamma \cdot L \cdot \Delta n}{n_g}$$
 (3.50)

meanwhile
$$\Delta n$$
 is defined as: $\Delta n = \frac{dn}{dN} \left(N'_{av} - N_{ref} \right)$ (3.51)

where N'_{av} - average carrier density along the whole cavity;

 $N_{\it ref}$ - reference carrier value for zero phase shift.

$$\frac{dn}{dN} = -\frac{\alpha_H \cdot c_0 \cdot a}{4 \cdot \pi \cdot f_0} \tag{3.52}$$

 $\alpha_{\scriptscriptstyle H}$ -Henry's linewidth enhancement factor;

a - differential gain constant.

3.4.4 Spontaneous emission model

The spontaneous emission noise represents a current source in TLLM and can be described by equation 3.53 (the detailed explanation of this formula can be found in [3]).

$$\left\langle i^{2}\right\rangle =\frac{2\cdot\beta\cdot R(N)\cdot h\cdot f_{0}\cdot m^{2}\cdot S}{Z_{p}\cdot\Delta l}\tag{3.53}$$

 β - spontaneous coupling coefficient;

R(N) - recombination rate;

h - Planck's constant;

 f_0 - lasing frequency;

m - unity of constant of unit length for the dimensional correctness;

S - S-section model;

 Z_n - wave impedance;

 Δl - unit section of length.

This mean square value from the equation above can be simulated by Gaussian random number generator. Moreover, the distributive model of the spontaneous emission noise can be fulfilled in TLLM by locating the current source along the model, where the local carrier concentration is evaluated (figure 3.16) [3].

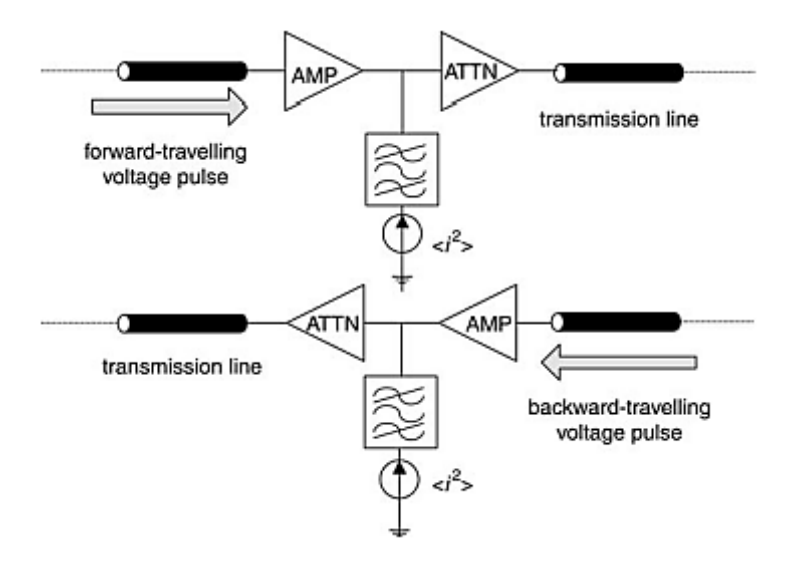


Figure 3.16 – Presentation of one section of distributed spontaneous emission model

3.5 Laser's parameters

The previous chapters of the basic theory and methodology of the TLLM fulfillment led to complete information which is required to the simulation of the laser-transmitter by TLLM on a computer. Moreover, it is necessary to consider other additional parameters of the laser, which are shown in the Table 3.3.

Table 3.3 – Parameters of the laser

Parameter	Value
Cavity length, L	300 µm
Number of sections (also modes), M	23
Active region thickness, d	0.1 <i>µm</i>
Active region width, w	5 μm
Effective index, $n_{\it eff}$ and Group index, $n_{\it g}$	3.4; 4
Time step, ΔT	174 fs
Wave impedance, Z_P	130 Ohms
Internal attenuation factor, $lpha_{ ext{int}}$	$70.0 \ cm^{-1}$
Carrier lifetime, τ_s	10 ns
Radiative recombination coefficient, B_0	$0.6 \times 10^{-16} \ m^3 s^{-1}$
Radiative recombination coefficient, B_1	$1.1 \times 10^{-41} m^6 s^{-1}$
Auger recombination coefficient, C_{Aug}	$4.0 \times 10^{-41} \ m^6 s^{-1}$
Free-space lasing wavelength, λ_0	1.3 µm
Confinement factor, Γ	0.3
Spatial gain per unit inversion, a	$4.1 \times 10^{-16} \ cm^{-2}$
Transparency carrier density, N_0	$1.0 \times 10^{24} \ m^{-3}$
Power facet reflectivities, r	0.3
Linewidth enhancement factor, β_{lw}	5.6
Threshold carrier density (calculated), N_{th}	$1.8 \times 10^{24} \ m^{-3}$
Initial carrier density (to save time), N_i	$1.8 \times 10^{24} \ m^{-3}$
Internal threshold current (active layer), I_{th}	14.5 mA
Photon lifetime, τ_p	1.21 <i>ps</i>
Gain compression factor, ε	$6.7 \times 10^{-23} \ m^{-3}$
Bias current, I_b	18.8 <i>mA</i>
Modulation current, I _m	14.2 mA (1 dBm max . power)
Gain spectrum Q-factor	40
Spontaneous emission coupling factor, β_{SP}	1.0×10^{-5}
Spontaneous emission spectrum Q-factor	15

4 Results and Discussion

In this chapter more important laser characteristics obtained from the simulation in Matlab environment are shown. The detailed code implementation based on Fortran code by Wong and Ghafouri-Shiraz [5] is given in Appendix B.

The evaluation of laser performance is provided by large signal modulation. For this purpose, laser can be driven by short pulse generation or by direct modulation technique. Both methods are considered in the simulation.

The common approach to drive the laser is direct modulation, which presents an input signal as bias current and modulation current components [3]:

$$I(t) = I_b + I_m(t) \tag{4.1}$$

where I_b - DC bias current;

 $I_m(t)$ - modulation current;

In this case, lasing occurs in a linear manner because the 'output waveform follows the modulation current waveform' [3].

In a case of short pulse generation, there are several methods to realize it such as Q-switching, gain-switching and mode-locking. This thesis is assumed the gain-switching technique which describes as follows. The light output of the laser occurs when it is driven by pumping the current above threshold. This technique is implemented by RF sine-wave generator or by comb generator, which are shown in figures 4.1, 4.2 for the same 1.1 GHz frequency [3]. In first case, modulated waveform is sinusoidal as shown in formula 4.1, however takes into account nonlinear effect due to biased threshold level. In a second case, modulated waveform is rectangular where switch on state emits an optical pulse and vice versa no emission in switch off state.

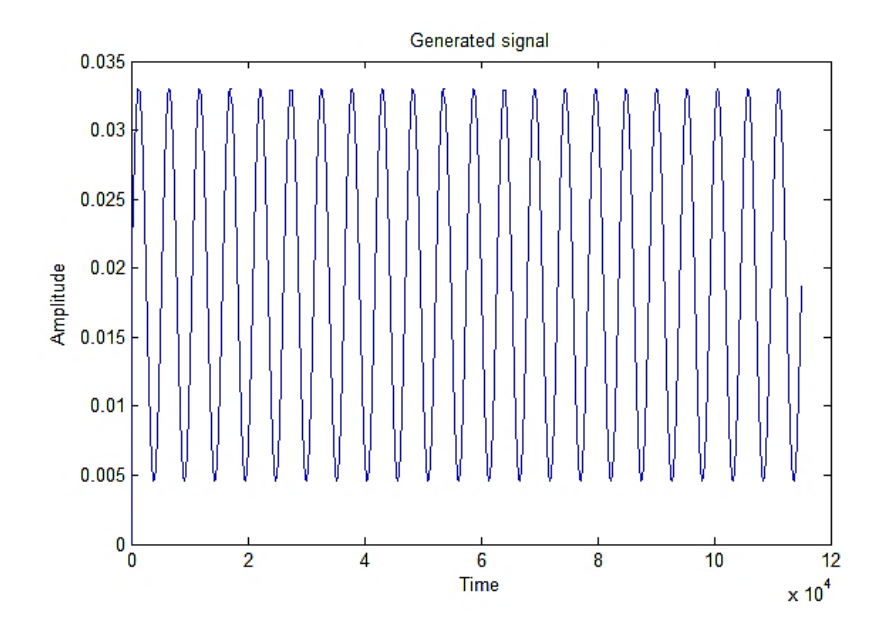


Figure 4.1 – Signal from sinusoidal generator

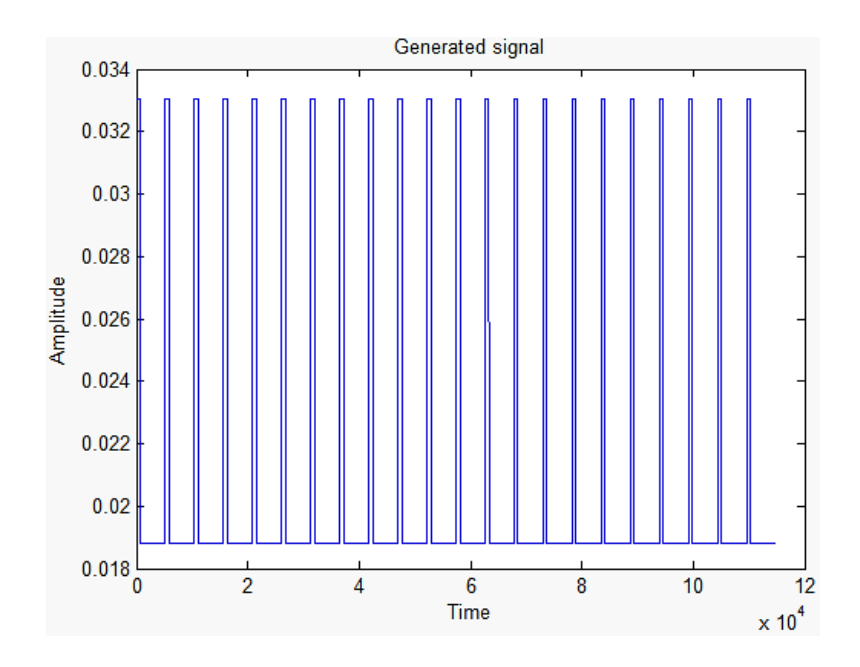


Figure 4.2 – Signal from rectangular generator

4.1 Return loss

First of all, the return loss S11 graphs based on TLLM simulation are shown for 1.1GHz and 6.6 GHz in figure 4.3 (Appendix B).

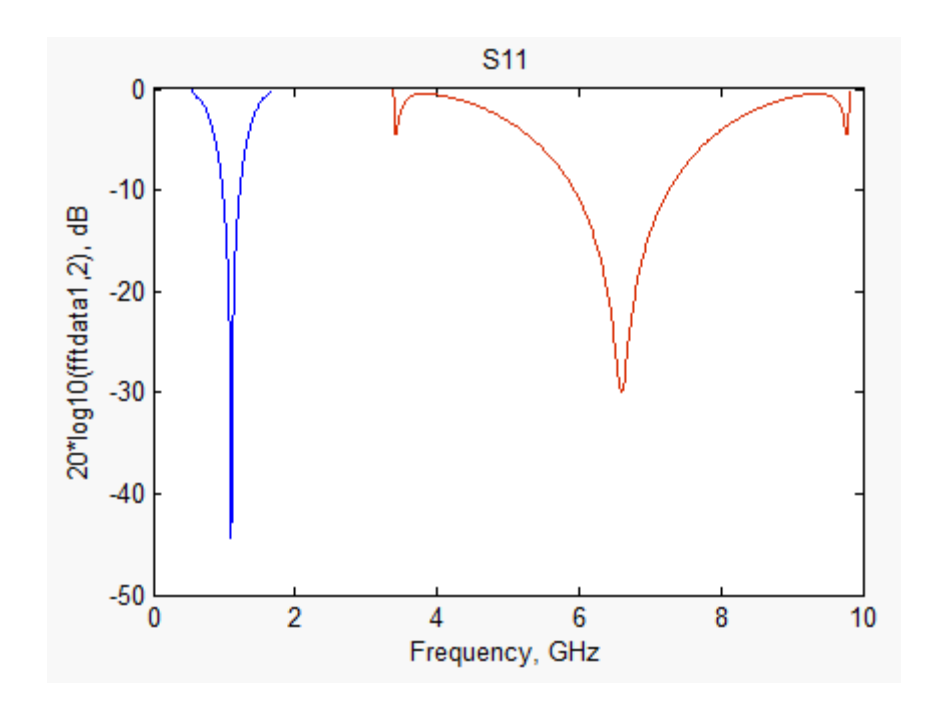


Figure 4.3 – S11 parameter for 1.1GHz and 6.6GHz respectively

This graph presents that S11 parameter for both cases have the same shape as shown in a AWR simulation tool, however the magnitudes of the return loss S11 for TLLM have different values. This can be fixed by more accurate TLLM (e.g. reducing the time step value Δt and by increasing the section number), however with a lack of computational time. All presented simulation results consider 115200 time step which takes around 30 minutes of simulation for Intel core i5 CPU.

4.2 Large signal analysis

The large signal analysis involves the evaluation of the laser performance including nonlinear properties. It can be investigated when laser biased above or below the threshold value known as harmonic generation by gain-switching. The following simulation considers all parameters from the Table 3.3, when laser driven by sinusoidal generator. The figure 4.4 presents gain-switched optical pulses for different subharmonic frequencies (1.1GHz, 2.2 GHz, 6.6 GHz). As it is shown, the higher power obtained at the subharmonic frequency 2.2GHz. Moreover, the pulse at the subharmonic frequency 1.1GHz is distorted and sometimes has the second product as it is shown at 12psec and 16.6psec. Moreover, power obtained at different subharmonic frequencies shows different amplitude, which is known as power diffusivity effect. As example, the optical pulse at subharmonic frequency 6.6GHz is almost not generated, because at the higher frequency the gain-switching process can not react so fast.

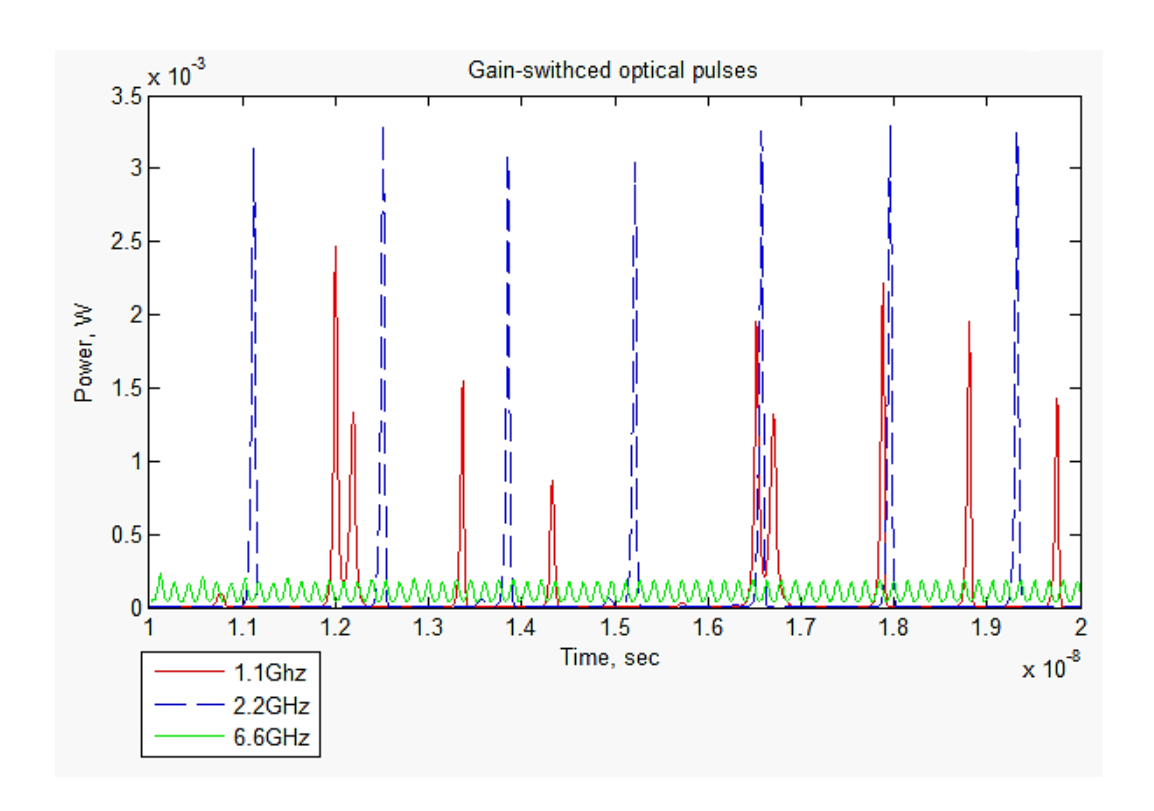


Figure 4.4 – Gain-switched optical pulses over 20psec

As it was mentioned before, the integrated model contains a matching network part. In order to evaluate its contribution to the laser performance the simulation of the table-averaged optical pulse at subharmonic frequency 2.2GHz is provided (fig. 4.5). The result of simulation shows improvement of the power by 0.1mW, which again confirms the relevance of the matching the source and the load.

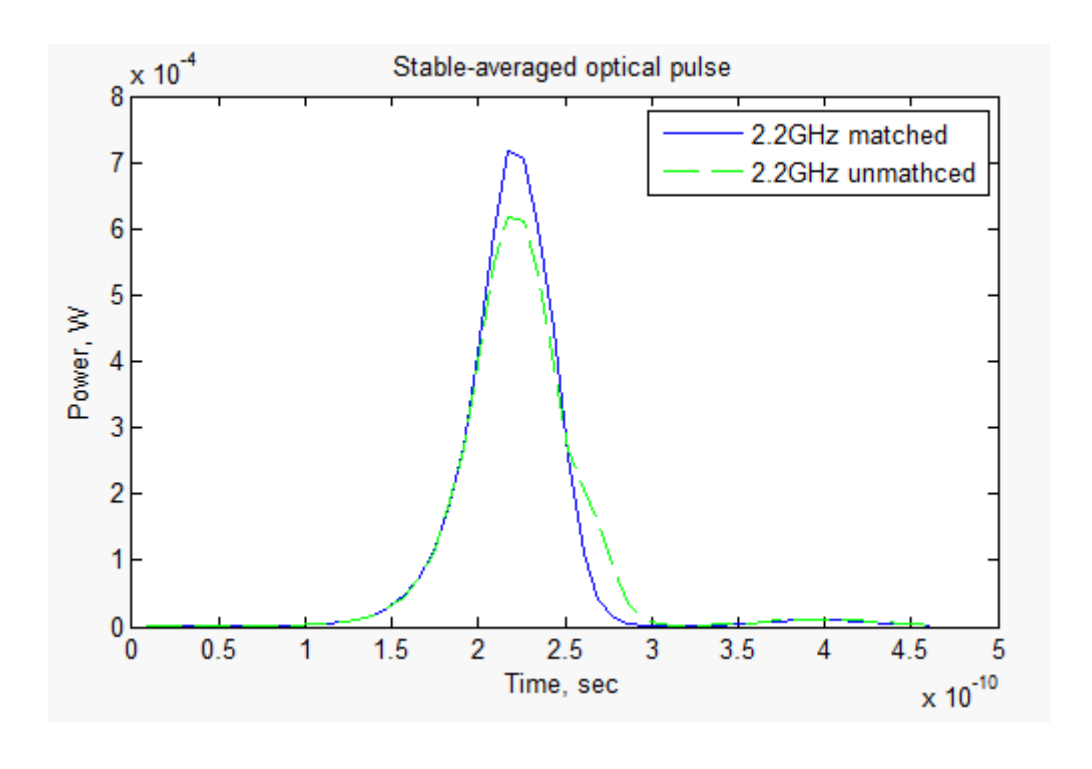


Figure 4.5 – Stable averaged optical pulse

Another simulation is produced with taking into account the linewidth enhancement factor, which plays an important role in frequency chirping as it is visually seen in figure 4.6, 4.7.

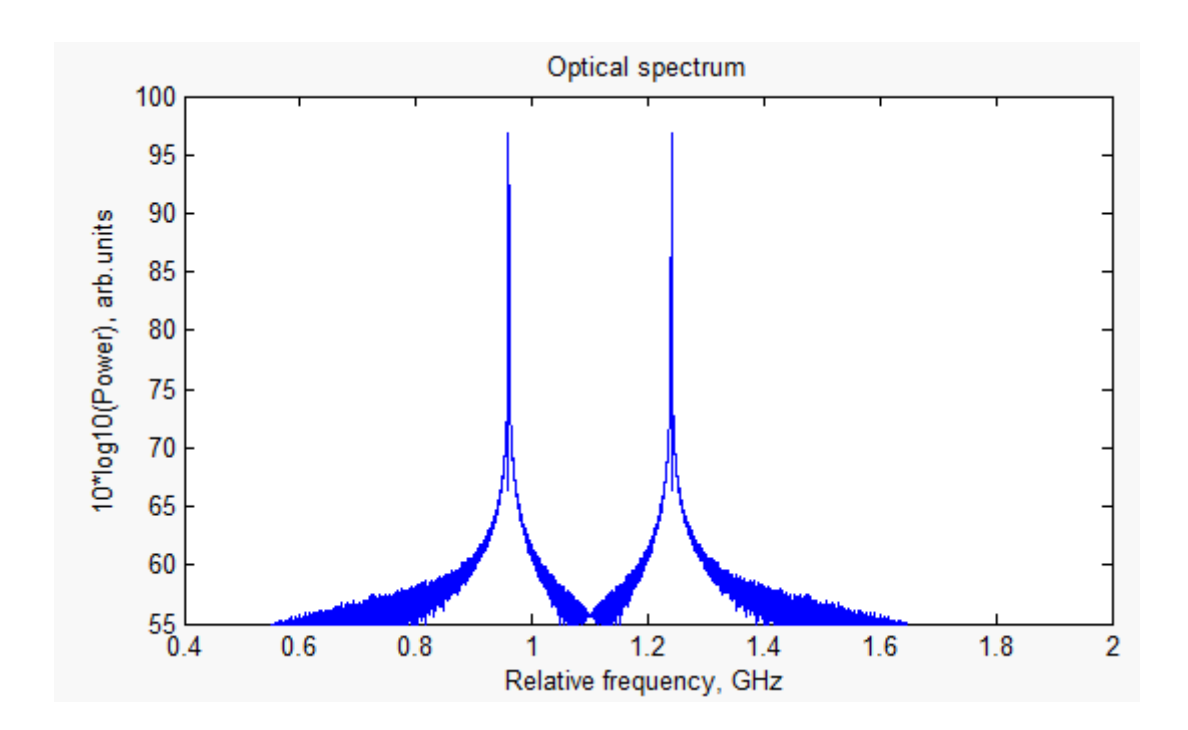


Figure 4.6 – Optical spectrum when gain-switched with linewidth enhancement factor equal 0

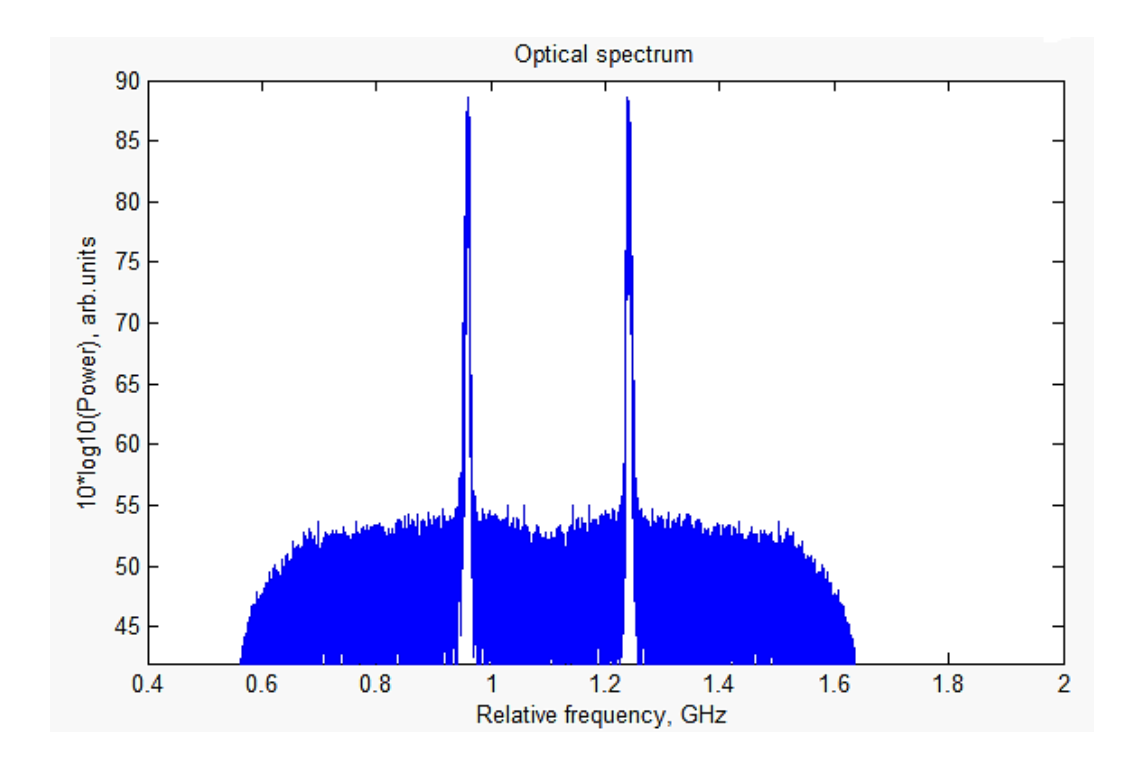


Figure 4.7 – Optical spectrum when gain-switched with linewidth enhancement factor equal 5.6

5 Conclusion

This thesis presents analysis of TLLM. The exploration of literature review, basic transmission-line and laser theory are discussed. Several results are in a good agreement with the original paper. Moreover, it is shown that optical processes play an important role in laser performance.

It is suggested a further improvement of the results as presented a small signal analysis and consideration another more enhanced type of matching network as a result that improvement can be achieved.

References

- [1] J.M. Senior (1992), Optical fiber communications: principles and practice. 2nd ed. New York; London: Prentice-Hall. pp.7-9, .281-315.
- [2] G. P. Agrawal (2002), Fiber-optic communication systems. 3rd ed. New York, N.Y: Wiley-Interscience, pp.75, 79-84.
- [3] H.Ghafouri-Shiraz (2004). The principles of semiconductor laser diodes and amplifiers. Imperial College Press, pp.413, 361-370, 473, 475,399, 403, 414-432, 382, 388,
- [4] K.C.Sum, N.J. Gomes (1998). Microwave-optoelectronic modelling approaches for semiconductor lasers. Optoelectronics, IEE Proceedings [online], volume:145, issue: 3, pp.141-146. Available from: http://ieeexplore.ieee.org/stamp/stamp.jsp?arnumber=710076
- [5] W.M.Wong, H.Ghafouri-Shiraz (1999), Integrate semiconductor laser-transmitter model for microwave-optoelectronic simulation based on transmission-line modelling. Optoelectronics, IEE Proceedings [online], volume: 146, issue: 4, pp.181-188. Available from: http://ieeexplore.ieee.org/xpl/articleDetails.jsp?reload=true&arnumber=819777 [Accessed 01 March 2014]
- [6] P. B. Johns, R. L. Beurle (1971), Numerical solution of 2-dimensional scattering problems using a transmission-line matrix [online], Electrical Engineers, Proceedings of the Institution of , volume:118 , issue: 9 , pp. 1203-1208. Available from: http://ieeexplore.ieee.org/stamp/stamp.jsp?tp=&arnumber=5251453
- [7] S. Akhtarzad (1975), Analysis of lossy microwave structures and microstrip resonators by the TLM method. PhD thesis, University of Nottingham [online], pp.1-98. Available from: http://etheses.nottingham.ac.uk/1770/1/482853.pdf [Accessed 01 August 2014]
- [8] W.J.R. Hoefer (1985), The Transmission-Line Matrix Method Theory and Applications. Microwave Theory and Techniques, IEEE Transactions on [online], volume:33, issue:10, pp.882-893. Available from: http://ieeexplore.ieee.org/stamp/stamp.jsp?tp=&arnumber=1133146 [Accessed 01 March 2014]
- [9] O. Berger, R. Heinzelmann, A. Stöhr et.al (1999). Modeling of the dynamics of multisection waveguide lasers. <u>Optical and Quantum Electronics</u> [online], <u>volume 31</u>, <u>issue 9-10</u>, <u>pp 1031-1045</u>. Available from:

- http://link.springer.com/article/10.1023/A%3A1006973000853 [Accessed 01 August 2014]
- [10] D. Marcuse (1984), Rate Equation Model of a Coupled-Cavity Laser. Quantum Electronics, IEEE Journal of [online], volume:20 , Issue: 2, pp. 166-176. Available from: http://ieeexplore.ieee.org/stamp/stamp.jsp?tp=&arnumber=1072360 [Accessed 01 August 2014]
- [11] J. Buus (1984), Principles of semiconductor laser modelling. Optoelectronics, IEE Proceedings J [online], volume 132, issue 1, pp. 42 51. Available from: http://digital-library.theiet.org/content/journals/10.1049/ip-j.1985.0010?crawler=true
- [12] T. Ohtoshi, K. Yamaguchi, C. Nagaoka et al (1986). A two-dimensional device simulator of semiconductor lasers. Solid State electronics [online], volume 30, issue 6, pp. 627-638. Available from: http://www.sciencedirect.com/science/article/pii/003811018790222X
- [13] G. Bjork, O. Nilsson (1987). A New Exact and Efficient Numerical Matrix Theory of Complicated Laser Structures: Properties of Asymmetric Phase-Shifted DFB Lasers. Lightwave Technology [online], volume: 5, issue:1, pp.140-146. Available from: http://ieeexplore.ieee.org/stamp/stamp.jsp?arnumber=1075402
- [14] M. G. Davis, R. F. O'Dowd (1994). A Transfer Matrix Method Based Large-Signal Dynamic Model for Multielectrode DFB Lasers. Quantum Electronics [online], volume: 30, issue: 11, pp. 2458 2466. Available from: http://ieeexplore.ieee.org/stamp/stamp.jsp?arnumber=333696
- [15] L. M. Zhang, J. E. Carroll (1992). Large-Signal Dynamic Model of the DFB Laser.

 Quantum Electronics [online], volume:28, issue: 3, pp.604-611. Available from:

 http://ieeexplore.ieee.org/stamp/stamp.jsp?arnumber=124984
- [16] D.D. Marcenac, J.E. Carroll (1993). Quantum-mechanical model for realistic Fabry-Perot lasers. Optoelectronics, IEE Proceedings J [online], volume:140 , issue: 3, pp.157-171. Available from: http://ieeexplore.ieee.org/stamp/stamp.jsp?arnumber=219413
- [17] A.J.Lowery (1989). Transmission-Line Modelling of semiconductor lasers: The Transmission-Line Laser Model. International Journal of Numerical Modelling: Electronic Networks, Devices and Fields [online], volume 2, issue 4, pp. 249–265, Available from: http://onlinelibrary.wiley.com/doi/10.1002/jnm.1660020408/abstract
- [18] D. A. B. Miller (1991). Huygens's wave propagation principle corrected. Optics Letters [online], volume: 16, issue: 18, pp. 1370-1372. Available from: http://www.opticsinfobase.org/ol/abstract.cfm?uri=ol-16-18-1370

- [19] Invocom website. Available from:

 http://www.invocom.et.put.poznan.pl/~invocom/C/P1-9/swiatlowody_en/p1
 1_6_5.htm
- [20] R. S. Tucker, I. P. Kaminow (1984). High-Frequency Characteristics of Directly Modulated InGaAsP Ridge Waveguide and Buried Heterostructure Lasers. Lightwave Technology, Journal of [online], volume:2, issue: 4, pp. 385-393. Available from: http://ieeexplore.ieee.org/stamp/stamp.jsp?arnumber=1073654
- [21] H. L. Martinez-Reyes, J. A. Reynoso-Hernandez, F. J. Mendieta (1999). DC and RF techniques for computing the series resistance of the equivalent electrical circuit for semiconductor lasers. Microwave and Optical Technology Letters [online], volume 20, issue 4, pp. 258–261. Available from: http://onlinelibrary.wiley.com/doi/10.1002/%28SICI%291098-2760%2819990220%2920:4%3C258::AID-MOP10%3E3.0.CO;2-A/pdf
- [22] H. Elkadi, J. P. Vilcot, S. Maricot, and D. Decoster (1990). Microwave circuit modeling for semiconductor lasers under large and small signal conditions. Microwave and Optical Technology Letters [online], volume 3, issue 11, pp. 379-382. Available from: http://onlinelibrary.wiley.com/doi/10.1002/mop.4650031102/abstract
- [23] X. Jin, S. L. Chuang (2001). Microwave Modulation of a Quantum-Well Laser with and without External Optical Injection. Photonics Technology Letters [online], volume: 13, issue: 7, pp. 648-650. Available from: http://ieeexplore.ieee.org/stamp/stamp.jsp?tp=&arnumber=930402
- [24] O. H. Anton, D. Patel, C. S. Menoni et al (2005). Frequency Response of Strain-Compensated InGaAsN–GaAsP–GaAs SQW Lasers. Selected Topics in Quantum Electronics [online], IEEE Journal of volume: 11, issue: 5, pp. 1079-1088. Available from: http://ieeexplore.ieee.org/stamp/stamp.jsp?tp=&arnumber=1564045
- [25] Y. Ou, J. S. Gustavsson, P. Westbergh et.al (2009). Impedance Characteristics and Parasitic Speed Limitations of High-Speed 850-nm VCSELs. Photonics Technology Letters [online], volume:21 , issue: 24, pp. 1840. Available from: http://ieeexplore.ieee.org/stamp/stamp.jsp?tp=&arnumber=5291742
- [26] D. M. Pozar (2012). Microwave engineering. 4th ed. Hoboken, N.J.: Wiley, pp.228-233.
- [27] A. Ghiasi, A. Gopinath (1990). Novel Wide-Bandwidth Matching Technique for Laser Diodes. Microwave Theory and Techniques [online], IEEE Transactions on volume: 38, issue: 5, p. 674. Available from: http://ieeexplore.ieee.org/stamp/stamp.jsp?tp=&arnumber=54940

- [28] S. Maricot, J. P. Vilcot, D. Decoster et.al. (1992, November). Monolithic Integration of Optoelectronic Devices with Reactive Matching Networks for Microwave Applications. Photonics Technology Letters [online], volume:4, issue: 11, pp. 1248-1250. Available from: http://ieeexplore.ieee.org/stamp/stamp.jsp?arnumber=166957
- [29] Laboratory tutorials. Available from : http://www.google.co.uk/url?sa=t&rct=j&q=&esrc=s&source=web&cd=1&ved=0CB8QFjAA&url=http
 wdid%252F%2Fwww.dii.unisi.it%2Flist.php%3Fid%3D11%26dir%3D.%252FFAC%252Fdidattica%252Fma
 tdid%252F%26download%3D727.doc&ei=M67vU7HvDcS ygOljYGYDA&usg=AFQjCNGguecbTRinRLq5
 ACUOwDjVO5qWlQ&bvm=bv.73231344,d.bGE
- [30] A.J. Lowery (1987). New dynamic semiconductor laser model based on the transmission-line modelling method. Optoelectronics, IEE Proceedings J [online], volume:134, issue: 5, pp.281-289. Available from: http://ieeexplore.ieee.org/xpls/abs_all.jsp?arnumber=4644417
- [31] A.J. Lowery (1988). Model for multimode picosecond dynamic laser chirp based on transmission line laser model. Optoelectronics, IEE Proceedings J [online], volume: 135, issue: 2, pp. 126-132. Available from: http://ieeexplore.ieee.org/xpls/abs_all.jsp?arnumber=6846
- [32] A.J. Lowery (1989). Dynamic modelling of distributed feedback lasers using scattering matrices. Electronics Letters [online], volume: 25, issue: 19, pp. 1307-1308. Available from: http://ieeexplore.ieee.org/stamp/stamp.jsp?arnumber=46196
- [33] L.Hairong, H. Ghafouri-Shiraz (2004, January). Application of the transmission line laser model in analysis of multiple-phase-shift DFB lasers. Microwave and Optical Technology Letters [online], volume 40, issue 1, p. 51. Available from: http://onlinelibrary.wiley.com/doi/10.1002/mop.11283/pdf
- [34] A.J. Lowery (1992, June). Transmission-line laser modelling of semiconductor laser amplified optical communications systems. Optoelectronics [online], IEE Proceedings J volume: 139, Issue: 3, p.180. Available from: http://ieeexplore.ieee.org/stamp/stamp.jsp?arnumber=144788
- [35] T. Shu, Y. Yu (2011). Modeling of Tunable DBRs Lasers Based on Transmission-Line Laser Model. Journal of Physics: Conference Series [online], volume 276 number 1, p. 2. Available from: http://iopscience.iop.org/1742-6596_276_1_012088.pdf
- [36] J. Bandler, P. Johns, M. Rizk (1977, July). Transmission-line modeling and sensitivity evaluation for lumped network simulation and design in the time domain. Journal of the Franklin Institute [online], volume 304, issue 1, pp. 15–32. Available

from: http://ac.els-cdn.com/0016003277901041/1-s2.0-0016003277901041-main.pdf? tid=80f8abae-2701-11e4-a983-00000aacb362&acdnat=1408384994_96f657602c5cbcf3138a1a4a58238453

[37] C. Peucheret (2011, July).Direct Current Modulation of Semiconductor Lasers. p.8 http://web-files.ait.dtu.dk/cpeu/download/34130_E2011_CPEU_DML_Sim.pdf

Appendix A

This short program is calculated the required values for the matching network part.

```
%Parameter values used in electrical parasitics network
                              %bondwire resistance
Rp = 1;
Lp = 0.63*power(10,-9);
                              %Bondwire inductance
Cp = 0.23*power(10,-12);
                              %Stand-off shunt capacitance
Rsub = 1.5;
                              %Chip substrate resistance
Cs = 8*power(10,-12);
                              %Shunt parasitic capacitance
Rs = 5.5;
                              %Chip series resistance
Csc = 2*power(10,-12);
                              %Space-charge capacitance
Rld = 2;
                              %Forward bias resistance
Rin = 50;
                              %Generator resistance
%Define the load impedance (impedance of the parasitics network)
f0=6.6*10^9;
Z11=Rsub+(1/(1i*2*pi*f0*Cs));
Z22 = (Z11*Rs) / (Z11+Rs);
Z33=Rp+(1i*2*pi*f0*Lp);
Z44=Z22+Z33;
Z55=1/(1i*2*pi*f0*Cp);
ZL=(Z44*Z55)/(Z44+Z55);
%Define Cm and Lm parameters for the matching network
%1st case
f1=1.1*10^9;
Z0=50;
R11=5.9916;
X11=2.8562;
X11=sqrt(Rl1*(Z0-Rl1))-Xl1;
X22=-sqrt(Rl1*(Z0-Rl1))-Xl1;
B11=sqrt((Z0-Rl1)/Rl1)/Z0;
B22 = -sqrt((Z0 - R11)/R11)/Z0;
C11=-1/(2*pi*f1*X11);
C22=-1/(2*pi*f1*X22);
L11=-1/(2*pi*f1*B11);
L22=-1/(2*pi*f1*B22);
%2d case
f2=6.6*10^9;
Z0=50;
R12=4.8;
X12=31.4;
B33 = (X12 + (sqrt(R12/Z0) * sqrt(R12^2 + X12^2 - Z0*R12))) / (R12^2 + X12^2);
B44 = (X12 - (sqrt(R12/Z0) * sqrt(R12^2 + X12^2 - Z0*R12))) / (R12^2 + X12^2);
X33 = (1/B33) + ((X12*Z0)/R12) - (Z0/(B33*R12));
X44 = (1/B44) + ((X12*Z0)/R12) - (Z0/(B44*R12));
C33=B33/(2*pi*f2);
C44=B44/(2*pi*f2);
L33=X33/(2*pi*f2);
L44=X44/(2*pi*f2);
```

Appendix B

The following program considers simulation of laser based on TLLM. It includes *Main* program, which accesses to subprogram such as *Parasitalgorithm, Calccarrdens, Calcphotdens, Matgain, Spontemissnoise, Scattalgorithm, Connalgorithm.*

Main

```
%This is the main program for the laser-transmitter model based on TLLM
 %DEFINE GLOBAL VARIABLES
 global dirn maxsec scrf
 dirn=2:
 maxsec=23; %number of sections
 scrf=2;
 % matrix notations
 global refl %reflected
global inci %incident
global bbb %backward
global bbb
global aaa
                      %forward
 % universal constants
global qelectron %electron charge
global planck %Planck's constant
global co %speed of light
 global co
 % laser parameters
global neff %effective index
global fo %free-space lasing frequency
global beta %spontaneous emission coupling factor
global zp %wave impedance
global ts %carrier lifetime
 global ts
 global attn
                         %attenuation
                      %group index
%cavity length
%gain compression factor
%power facet reflectivities
%power facet reflectivities
%transparency carrier density
 global ngrp
 global len
global gcomp
 global r2
 global r1
 global no
global wid %active region width %active region thickness global nth %threshold carrier densit global mirlos %mirror loss global linenfc %linewidth enhance global vol % *****
                         %spatial gain per unit inversion
                           %threshold carrier density
                           %linewidth enhancement factor
 global auger
                           %Auger recombination coefficient
global rad_1 %radiative recombination coefficient global rad_0 %radiative recombination coefficient
 global stim emis
```

```
% sampling time
global fsamp
                    %sampling frequency
global fnyq
                    %Nyquist frequency
global maxtime
global dl
                    %one section length
global dt
                    %time step
% propagation
global omega
                    %angular frequency
global pbeta
                    %propagation constant
% modulation
global i mod
                    %modulation current (1dBm max.power)
global freq rf
                    %modulation frequency
% bias
global dcinj
                    %bias current
% sample power
global pstop
global pstart
% sample carrier
global cstop
global cstart
% time elapsed before injecting signal
global time inj
% added to initialise intrinsic data in modules
global para 1
global spon 1
global connect 1
global findss 1
global s11
global s11 n
global s21
global s21 n
global injpr
global injpr n
global pul1
global pull n
global rf11a
global rf11a n
global rf11b
global rf11b n
global pul2
global pul2 n
global sv
global svc
global svl
global nis
global pss
global qnn
% initialisation
injpr n=0;
s11 n=0;
pul\overline{1} n=0;
rf11a n=0;
rf11b n=0;
```

```
pul2 n=0;
s21 = 0;
para 1=0;
spon 1=0;
connect 1=0;
findss 1=0;
% matrix notations
aaa=1; %forward
bbb=2; %backward
inci=1; %incident
refl=2; %reflected
% universal constants
co=3e8;
                        %speed of light
planck=6.6260755e-34;
                        %Planck's constant
qelectron=1.60217733e-19; %electron charge
boltzmann=1.380658e-23;
                        %Boltzmann constant
kelvin=290;
                        %temperature
% laser parameters
%len=200e-6;
                        %cavity length
len=300e-6;
dl=len/maxsec;
                        %one section length
%dthic=0.2e-6;
                        %active region thickness
dthic=0.1e-6;
wid=5e-6;
                        %active region width
vol=dthic*wid*len;
                        %volume of the laser
%neff=3.3;
                         %effective index
neff=3.4;
                        %group index
ngrp=4;
dt=(len/maxsec)*ngrp/co; %time step
zp=120*pi*ngrp/(neff^2); %wave impedance
%loss_scat=7500;
                        %internal attenuation factor (7*10^3 because of the
units conversion)
loss scat=7000;
attn=exp(-loss scat*dl/2); %attenuation
                        %carrier lifetime
ts=10e-9;
rad 0=0.6e-16;
                        %radiative recombination coefficient
                       %radiative recombination coefficient
rad 1=1.1e-41;
auger=4.0e-41;
                        %Auger recombination coefficient
wvlno=1.3251e-6;
                        %free-space lasing wavelength
% actual lasing freq (no shift)
fo=co/wvlno;
                     %free-space lasing frequency
omega=2*pi*fo;
                        %angular frequency
pbeta=omega/(co/ngrp); %propagation constant
% note that group velocity=phase velocity=dl/dt in tllm
%pbeta=omega/(dl/dt);
%cfn=0.2385;
                        %confinement factor
cfn=0.3;
aa=4.1e-20;
                       %spatial gain per unit inversion (it is important to
note that the power (-20) because of units conversion cm^{(-2)-m}(-4)
                        %transparency carrier density
no=1.0e24;
```

```
%r1=0.32;
                       %power facet reflectivity
%r2=0.32;
                       %power facet reflectivity
r1=0.3;
r2=0.3:
linenfc=5.6;
                       %linewidth enhancement factor
mirlos=1/(2*len)*log(1/(r1*r2));
                                                       %mirror loss
(% be careful of divide by zero when r1 and r2 = 0)
nth=no+(mirlos+loss scat)/(aa*cfn);
                                                       %threshold
carrier density (is required for the case when chirp is taken into account
                                                       % or when
gain peak is carrier dependent (np=nth))
ith=qelectron*vol*(nth/ts +(rad 0-rad 1*nth)*nth^2 +auger*nth^3); %internal
threshold current
phlt=1/(co/ngrp*(mirlos+loss_scat));
                                                       %photon
lifetime
np=nth;
                                                       %initial
carrier density
aa2=4e5*1.0e2;
                                                       %describes
width of gain curve
aa3=1.4e-20*gelectron*1e-6;
                                                       %describes
shift in gain peak with carrier density
fint=1/(4*dt);
gcomp=6.7e-23;
                %freq of interest - for accurate fp-gain curve
                %gain compression factor
fnyq=1/(2*dt);
                %Nyquist frequency
fsamp=1/dt;
                %sampling frequency
% max iterations
maxtime=20e-9/dt;
%maxtime=30e-9/dt;
pstart=10e-9/dt;
pstop=maxtime-1.0;
cstart=pstart;
cstop=maxtime;
time inj=0;
% if electrical parasitics network is included choose y(=1) if not choose n(=0)]
elpar=1;
% type of modulation (in this model one type of modulation by setting 1 instead
of zero can be initialised)
                %rf modulation
rfsin=1;
combgen=0;
                %comb generator
dcinj=1.3*ith; %bias current
i \mod 14.2e-3;
                %modulation current (1dBm max.power)
%i mod=0;
fwhmcmb=100e-12/dt; %full-width half minimum of stable-averaged optical pulse
freq rf=6.6e9;
                %modulation freq
%spontaneous emission coupling factor
beta=1e-5;
nn_i=1.4e16;
               %intrinsic carrier density (required when junction
resistance Rd is a carrier dependent)
stim emis=0;
               %stimulated emission
```

```
% initialise array
for sec=1:maxsec
sv(aaa, sec, inci) = 0;
                       %voltage on the main line
sv(aaa, sec, refl) = 0;
sv(bbb, sec, inci) =0;
sv(bbb, sec, refl) = 0;
svc(aaa, sec, inci) = 0;
                       %voltage on the capacitive line
svc(aaa, sec, refl) = 0;
svc(bbb, sec, inci) = 0;
svc(bbb, sec, refl) = 0;
svl(aaa, sec, inci) = 0;
                       %voltage on the inductive line
svl(aaa, sec, refl) = 0;
svl(bbb, sec, inci) = 0;
svl(bbb, sec, refl) = 0;
nis(sec,inci)=0;
nis(sec, refl) = 0;
pss(sec) = 0;
qnn(sec)=nth;
a1=0;
a2=0;
a3=0;
a4=0;
hpvl(aaa, sec, inci) = 0;
                       %pulse on the high-pass filter (HPF)
hpvl(bbb, sec, refl)=0;
hpvl(aaa, sec, inci) =0;
hpvl(bbb, sec, refl) = 0;
hpv(aaa, sec, inci) = 0;
hpv(bbb, sec, refl) = 0;
hpv(aaa, sec, inci) = 0;
hpv(bbb, sec, refl) = 0;
lpvc(aaa, sec, inci) = 0;
                       %pulse on the low-pass filter (LPF)
lpvc(bbb, sec, refl) = 0;
lpvc(aaa, sec, inci) = 0;
lpvc(bbb, sec, refl) = 0;
lpv(aaa, sec, inci) = 0;
lpv(bbb, sec, refl) = 0;
lpv(aaa, sec, inci) = 0;
lpv(bbb, sec, refl) = 0;
end
% initialise variables
                      %input dirac delta pulse
sv(aaa,1,inci)=1;
trigger=0;
oldtrig=0;
tcmb=0;
df=co/(2*ngrp*len);
%output parameters to the txt file
fid=fopen('outputparam.txt','w');
fprintf(fid,'%s\n',[ 'laser cavity parameters' ])
fprintf(fid,'%s\n',[ 'cavity length =' num2str(len*1.0d6) 'mum' ])
fprintf(fid,'%s\n',[ 'photon lifetime =' num2str(phlt*1.0d12) 'ps' ])
fprintf(fid,'%s\n',[ num2str(maxsec) 'sections/modes'])
fprintf(fid,'%s\n',[ 'length of one section =' num2str(dl*1.0d6) 'mum' ])
```

```
fprintf(fid, '%s\n', [ 'active region thickness = ' num2str(dthic*1.0d6) 'mum' ])
fprintf(fid, '%s\n', [ 'active region width = ' num2str(wid*1.0d6) 'mum' ])
fprintf(fid,'%s\n',[ 'effective index =' num2str(neff) 'unitless' ])
fprintf(fid,'%s\n',[ 'group index =' num2str( ngrp) 'unitless' ])
fprintf(fid,'%s\n',[ 'confinement factor =' num2str(cfn) 'unitless' ])
fprintf(fid,'%s\n',[ 'wave impedance =' num2str(zp) 'ohms' ])
fprintf(fid,'%s\n',[ 'free-space lasing wavelength(carrier indep) ='
num2str(wvlno*1.0d6) 'mum'])
fprintf(fid,'%s\n',[ 'free spectral range(no chirp) =' num2str(df*1.0d-12)
'thz'])
fprintf(fid,'%s\n',['facet power reflectivity(left)=' num2str(r1) 'unitless' ])
fprintf(fid,'%s\n',['facet power reflectivity(right)=' num2str(r2) 'unitless'
fprintf(fid,'%s\n',[ 'linewid enhanc factor =' num2str(linenfc) 'unitless'])
fprintf(fid,'%s\n',[' '])
fprintf(fid,'%s\n',[ 'recombination-rate coefficients' ])
fprintf(fid,'%s\n',['carrier lifetime(carrier indep) =' num2str(ts*1.0d9) 'ns'
1)
fprintf(fid,'%s\n',[ 'radiative recomb coeff =' num2str(rad 0*1.0d16) '*1e-16
fprintf(fid,'%s\n',[ 'radiative recomb coeff =' num2str(rad 1*1.0d41) '*1e-41
m6s-1'])
fprintf(fid,'%s\n',[ 'auger recomb coeff =' num2str(auger*1.0d41) '*1e-41 m6s-
1'])
fprintf(fid,'%s\n',[' '])
fprintf(fid,'%s\n',[ 'gain/loss parameters ' ])
fprintf(fid,'%s\n',[ 'internal attenuation factor =' num2str(loss scat*1.0d-2)
'cm-1'1)
fprintf(fid,'%s\n',[ 'spatial gain per unit inversion =' num2str(aa*1.0d20)
'*1e-16 cm-2'])
fprintf(fid, '%s\n', [ 'gain compression factor = ' num2str(gcomp*1.0d23) '*1e-23' | fprintf(fid, '%s\n', [ 'gain compression factor = ' num2str(gcomp*1.0d23) '*1e-23' | fprintf(fid, '%s\n', [ 'gain compression factor = ' num2str(gcomp*1.0d23) '*1e-23' | fprintf(fid, '%s\n', [ 'gain compression factor = ' num2str(gcomp*1.0d23) '*1e-23' | fprintf(fid, '%s\n', [ 'gain compression factor = ' num2str(gcomp*1.0d23) '*1e-23' | fprintf(fid, '%s\n', [ 'gain compression factor = ' num2str(gcomp*1.0d23) '*1e-23' | fprintf(fid, '%s\n', [ 'gain compression factor = ' num2str(gcomp*1.0d23) '*1e-23' | fprintf(fid, '%s\n', [ 'gain compression factor = ' num2str(gcomp*1.0d23) '*1e-23' | fprintf(fid, '%s\n', [ 'gain compression factor = ' num2str(gcomp*1.0d23) '*1e-23' | fprintf(fid, '%s\n', [ 'gain compression factor = ' num2str(gcomp*1.0d23) '*1e-23' | fprintf(fid, '%s\n', [ 'gain compression factor = ' num2str(gcomp*1.0d23) '*1e-23' | fprintf(fid, '%s\n', [ 'gain compression factor = ' num2str(gcomp*1.0d23) '*1e-23' | fprintf(fid, 'gain compression factor = ' num2str(gcomp*1.0d23) '*1e-23' | fprintf(fid, 'gain compression factor = ' num2str(gcomp*1.0d23) '*1e-23' | fprintf(fid, 'gain compression factor = ' num2str(gcomp*1.0d23) '*1e-23' | fprintf(fid, 'gain compression factor = ' num2str(gcomp*1.0d23) '*1e-23' | fprintf(fid, 'gain compression factor = ' num2str(gcomp*1.0d23) '*1e-23' | fprintf(fid, 'gain compression factor = ' num2str(gcomp*1.0d23) '*1e-23' | fprintf(fid, 'gain compression factor = ' num2str(gcomp*1.0d23) '*1e-23' | fprintf(fid, 'gain compression factor = ' num2str(gcomp*1.0d23) '*1e-23' | fprintf(fid, 'gain compression factor = ' num2str(gcomp*1.0d23) '*1e-23' | fprintf(fid, 'gain compression factor = ' num2str(gcomp*1.0d23) '*1e-23' | fprintf(fid, 'gain compression factor = ' num2str(gcomp*1.0d23) '*1e-23' | fprintf(fid, 'gain compression factor = ' num2str(gcomp*1.0d23) '*1e-23' | fprintf(fid, 'gain compression factor = ' num2str(gcomp*1.0d23) '*1e-23' | fprintf(fid, 'gain compression factor = ' num2str
m-3!1)
fprintf(fid,'%s\n',[' '])
fprintf(fid,'%s\n',[ 'sampling rates ' ])
fprintf(fid,'%s\n',[ 'delay time =' num2str(dt*1.0d15) 'fs' ])
fprintf(fid,'%s\n',['nyquist frequency(bandwidth) =' num2str(fnyq*1.0d-12)
'thz'])
fprintf(fid,'%s\n',['sampling frequency(2*nyquist) =' num2str(fsamp*1.0d-12)
'thz'])
fprintf(fid,'%s\n',[ 'model propagation constant = ' num2str(pbeta*1.0d-6) '*1e6
radian m-1 s'])
fprintf(fid,'%s\n',[' '])
fprintf(fid,'%s\n',['spontaneous emission'])
fprintf(fid,'%s\n',[ 'spont emis coupling factor =' num2str(beta*1d6) '*1e-6
unitless'])
fprintf(fid,'%s\n',[' '])
fprintf(fid,'%s\n',[ 'operating conditions' ])
fprintf(fid,'%s\n',[ 'maximum laser time = ' num2str(maxtime*dt*1.0d9) 'nsec'])
fprintf(fid,'%s\n',[ 'transparency carrier density =' num2str(no*1.0d-24)
'*1e24 m-3'])
fprintf(fid,'%s\n',['threshold carrier density (calc) =' num2str(nth*1.0d-24)
'*1e24 m-3'])
fprintf(fid,'%s\n',['initial carrier density =' num2str(qnn(1)*1.0d-24) '*1e24
fprintf(fid, '%s\n', [ 'reference carrier density = ' num2str(np*1.0d-24) '*1e24 m-
3'1)
fprintf(fid,'%s\n',['threshold current (active layer) = num2str(ith*1.0d3)
'ma'])
fprintf(fid,'%s\n',['bias current(step) =' num2str(dcinj*1.0d3) ' ma'])
fprintf(fid,'%s\n',[ 'modulation current =' num2str(i mod*1.0d3) ' ma'])
%fprintf(fid,'%s\n',[ 'gain coeff 2 =' num2str(aa2*1.0d-2*1.0d-5) '*1e5 cm-1'])
%fprintf(fid,'%s\n',[ 'gain coeff 3 ='%num2str(aa3/qelectron*1.0d6*1.0d20)'*1e-
20 cm3'])
```

```
f(id, 'sn', [ ' fwhm(wavelength) of spont emis line='fwhmsp*1.0d6]
'mum'])
%fprintf(fid,'%s\n',[ 'spont emis line q-factor='nqfac' unitless'])
%fprintf(fid,'%s\n',[ 'spont emis line q-factor (down-converted)='dcnqfac'
unitless'])
%fprintf(fid,'%s\n',[ 'band number='band' unitless'])
f(fid, 'ss\n', [ 'gain q-factor of one filter section='qfac' unitless'])
f(fid, 'ss\n', [ 'gain q-factor (down-converted)='dcqfac'sunitless'])
%fprintf(fid,'%s\n',[ 'gain q-factor (effective)='qeff'%unitless'])
fclose(fid)
% begin lasing; one iteration represents dt
for ptime=0:1:maxtime
%show timestep on the screen
if mod(ptime, 1000) < 1</pre>
disp(['timestep ' num2str(ptime) ' of ' num2str(maxtime)])
end
               %calculate average carrier density
avgnn=mean(qnn);
      %constant value of junction resistance
%rd=(2*boltzmann*kelvin/qelectron)*dt/(qelectron*vol*(avgnn-
nn i))*log(avgnn/nn i+1); %value of junction resistance when it carrier
dependent
% accurate fp-gain filter
dcfo=fint+aa3*(avgnn-np)/planck; % down-converted centre freq (carrier
dependent)
fwhmgs=2*qelectron/planck*sqrt( abs(aa*(avgnn-no)/aa2)); %fwhm of gain spectra
qeff=dcfo*3.14/fwhmgs; % effective q-factor
pp=1/(dcfo*dt); %define pp as
% accurate gain curve
band=26;
                                  %bandnumber
dcfo=fo-band*(1/dt);
                                  %independent gain peak
%dcfo=fo-band*(1/dt)+1.5d-12*(avgnn-nth)%carrier-dependent gain peak
%Parameters are passed to subroutine scatter
qfac=40;
                              %Q-factor of stubs
%qfac=100;
                              %O-factor of stubs
dcqfac=qfac*(1-band/(fo*dt));
                             %baseband O factor
                             %addmitances of inductive stub line
yl=dcqfac*tan(pi*dcfo*dt);
                           %addmitances of capacitive stub line
yc=dcqfac/tan(pi*dcfo*dt);
totaly=1+yc+yl;
                              %total addmitance of the stub
ngfac=15;
                              %effective Q-factor
```

```
dcngfac=ngfac*(1-band/(fo*dt));
                                  %baseband O factor
nyl=dcnqfac*tan(pi*dcfo*dt);
                                   %addmitances of inductive stub line
                                   %addmitances of capacitive stub line
nyc=dcnqfac/tan(pi*dcfo*dt);
ntotaly=1+yc+yl;
                                   %total addmitance of the stub
ffhp=2.467*pp-3.867;
fflp=0.050*pp;
hpyl= tan(pi*fint*dt)/ffhp;
                                   %high pass
lpyc= 1/(fflp*tan(pi*fint*dt));
                                   %low pass
hptotaly=1+hpyl;
lptotaly=1+lpyc;
% find gain
for sec=1:maxsec
if (qnn(sec) > no)
gamma(sec) = (cfn*aa*dl/2*(qnn(sec)-no)*(1/(1+gcomp*pss(sec)))); %gain model
% (1.0d0-gcomp*pss(sec)) )
temp10=gamma(sec);
pgain(sec) = \exp(temp10) - 1;
elseif (qnn(sec) <= no)</pre>
pgain(sec) = 0;
end
end
% contribution from optical interface (laser diode)
vd=(2*boltzmann*kelvin/qelectron)*log(avgnn/nn i+1);
% inject step input current (bypassing parasitics)
if (ptime <= 0)
inj=0*ith;
else
inj=dcinj;
end
% inject an impulse of 1 ps after steady-state; modulation response
%if ( (ptime>=115000) && (ptime<115000+1e-12/dt) )
%inj=inj+i mod;
%else
%inj=inj;
%end
% to send in modulation current after steady-state is reached
if (ptime >= time_inj)
% comb generator
if (combgen == 1)
trigger=sin(2*pi*freq rf*(ptime)*dt);
if (oldtrig <= 0)</pre>
if (trigger > 0)
tcmb=0;
end
end
tcmb=tcmb+1;
if (tcmb <= fwhmcmb)</pre>
inj=dcinj+i mod;
```

```
elseif (tcmb > fwhmcmb)
inj=dcinj;
end
oldtrig=trigger;
% rf modulation (phase offset is zero)
if (rfsin == 1)
inj=inj +i mod*sin(2*pi*freq rf*(ptime)*dt);
end
end
% tlm electrical parasitics
if (elpar == 1)
res1 = parasitalgorithm(ptime,rd,inj);
injpr n=injpr n+1;
injpr(injpr_n,1) = ptime;
injpr(injpr_n,2)=inj;
end
% call calccarrdens subprogramm (calculate carrier density value in each and
every section)
res2 = calccarrdens(ptime,inj,pss);
% call calcphotdens subprogramm (calculate photon density value in each and
every section)
res3 = calcphotdens(inj,gamma,ptime,sv);
% call accurate material gain
res4 = matgain(dcfo,qeff,a1,a2,a3,a4);
% call spontaneous emission subprogram
res5 = spontemissnoise(nyl,nyc,ntotaly,avgnn,a1,a3,a4,ptime,qnn);
% call scatter subprogram
res6 = scattalgorithm(yc,yl,totaly,pgain,nis,ptime);
% call connect subprogram
res7 = connalgorithm(avgnn,ptime);
end
%write the calculated (output) data to the txt file in order to get graphs from
these data
dlmwrite('injpr.txt',injpr);
                                    %data for getting injection impulse graph
dlmwrite('s11.txt',s11);
                                     %data for getting return loss graph
dlmwrite('s21.txt',s21);
dlmwrite('rf11b.txt',rf11b);
                                    %data for getting optical pulse graph
dlmwrite('rf11a.txt',rf11a);
                                    %data for the stable averaged pulse
dlmwrite('pul1.txt',pul1);
dlmwrite('pul2.txt',pul2);
```

Parasitics

```
% This subprogram takes into account parasitics and mathcin network part
function res = parasitalgorithm(para time,para rd,para inj)
%DEFINE GLOBAL VARIABLES
global scrf maxport maxsec para
global para 1
scrf=2;
maxport=3;
maxsec para=4 ;
% sampling time
global dt
% matrix notations
global refl
global inci
global bbb
global aaa
persistent v para
persistent vlmat
global para 1
global s11
global s11 n
global s21
global s21 n
% initialise
if para_1 == 0
para_1=1;
s11 = 0;
for sec=1:maxsec para
v para(inci,1,sec)=0;
v para(refl,1,sec)=0;
v para(inci,2,sec)=0;
v_para(refl,2,sec)=0;
v_para(inci, 3, sec) = 0;
v para(refl,3,sec)=0;
end
% matching network with lumped elements
vlmat(inci, 1) = 0;
vlmat(refl,1)=0;
vlmat(inci, 2) = 0;
vlmat(refl, 2) = 0;
vlmat(inci, 3) = 0;
```

```
vlmat(refl,3)=0;
end
% if matching network is included choose y(=1) if not choose n(=0)]
matched=1;
% electrical parasitics
% Resistance of the nodes (here only node 3 contains a loss TL)
R1n2=0:
R2n2=0;
R3n2=0;
R1n3=1;
R2n3=5.5;
R3n3=1.5;
Rm1=0;
Rm2 = 0;
Rm3 = 0;
%Initialise the required subharmonic frequency (manual change is required)
% matched at 1.1 ghz
%Lm=1.889e-9;
%Cm=8.04e-12;
% matched at 1.32 ghz
%Lm=2.2244e-9;
%Cm=6.3145e-12;
% matched at 1.65 ghz
%Lm=1.7795e-9;
%Cm=5.0516e-12;
% matched at 2.2 ghz
%Lm=1.3347e-9;
%Cm=3.7887e-12;
% matched at 3.3 ghz
Lm=0.8898e-9;
Cm=2.5258e-12;
% matched at 6.6 ghz (note! change position of 1 and c)
Cm=0.957e-12;
%Lm=2.173e-9;
Rin=50;
           %generator resistance
Csc=2e-12;
          %space charge capacitance
Lp=0.63e-9;
          %bondwire inductance
Cp=0.23e-12;
          %stand-off shunt capacitance
Cs=8.0e-12;
          %shunt parasitic capacitance
% ld impedance (real)
Rout=para rd;
%without matching (50 oh TL feeding the RF signal)
if (matched == 0)
```

```
Z1n2=Rin;
end
%with matching
% input port of electrical parasitics (choose Z1n2 with respecting with the
frequency)
if (matched == 1)
%Z1n2=Lm/dt;
                %matched below 6.6Hz
Z1n2=dt/(Cp/2); %matched at 6.6GHz (splitting the bondwire shunt cap into 2
parts)
end
% bondwire induct (link-line)
Z2n2=Lp/dt;
% stand-off shunt cap (stub-line)
Z3n2=dt/(2*Cp);
% bondwire induct (link-line)
Z1n3=Z2n2;
% space charge cap (link-line)
Z2n3=dt/Csc;
% shunt cap (stub-line)
Z3n3=dt/(2*Cs);
% matching reactive lumped elements
if (matched == 1)
%choose Z1m, Z3m with respecting with the frequency (manual change is required)
                    %matched below 6.6Hz
%7.1m=Rin:
                  %matched at 6.6GHz (inductive element changes position)
Z1m=Lm/dt;
Z2m=Z1n2;
23m = dt/(2*Cm);
                    %matched below 6.6Hz
Z3m=dt/(2*(Cp/2));
                  %matched at 6.6GHz
%Define the values of matrices
Pm1=Z1m/(Z1m+Rm1);
Pm2=Z2m/(Z2m+Rm2);
Pm3=Z3m/(Z3m+Rm3);
Rm11 = (Rm1 - Z1m) / (Rm1 + Z1m);
Rm22 = (Rm2 - Z2m) / (Rm2 + Z2m);
Rm33 = (Rm3 - Z3m) / (Rm3 + Z3m);
Zsm1=(Rm1+Z1m);
Zsm2=(Rm2+Z2m);
Zsm3=(Rm3+Z3m);
Cm=1/(Zsm1*Zsm2+Zsm1*Zsm3+Zsm2*Zsm3);
end
P1n2=Z1n2/(Z1n2+R1n2);
P2n2=Z2n2/(Z2n2+R2n2);
```

```
P3n2=Z3n2/(Z3n2+R3n2);
P1n3=Z1n3/(Z1n3+R1n3);
P2n3=Z2n3/(Z2n3+R2n3);
P3n3=Z3n3/(Z3n3+R3n3);
R11n2 = (R1n2 - Z1n2) / (R1n2 + Z1n2);
R22n2 = (R2n2 - Z2n2) / (R2n2 + Z2n2);
R33n2 = (R3n2 - Z3n2) / (R3n2 + Z3n2);
R11n3 = (R1n3 - Z1n3) / (R1n3 + Z1n3);
R22n3 = (R2n3 - Z2n3) / (R2n3 + Z2n3);
R33n3 = (R3n3 - Z3n3) / (R3n3 + Z3n3);
Zs1n2=(R1n2+Z1n2);
Zs2n2 = (R2n2 + Z2n2);
Zs3n2 = (R3n2 + Z3n2);
Zs1n3 = (R1n3 + Z1n3);
Zs2n3 = (R2n3 + Z2n3);
Zs3n3 = (R3n3 + Z3n3);
% common denominator
Cn2=1/(Zs1n2*Zs2n2+Zs1n2*Zs3n2+Zs2n2*Zs3n2);
Cn3=1/(Zs1n3*Zs2n3+Zs1n3*Zs3n3+Zs2n3*Zs3n3);
% incident voltage wave to tlm parasitics
%v para(inci,1,1)=1;
v para(inci,1,1)=para inj*Rin/2;
% Note: Power delivered = (1/2/Rin)*[v para(inci,1,1)^2]
% if para inj=14.2mA(use peak amplitude); Rin=50ohms; then Power = 1dBm
% by convention, V source = V means V source = |V| * exp(j*w*t)
               write (*,*) 'v para (inci, 1, 1) = ', v para (inci, 1, 1)
v para(inci,2,4)=0; %no incident voltage wave from intrinsic laser diode
% scatter
§_____
% without matching network
if (matched == 0)
v para(refl, 2, 1) = (2*Z1n2/(Rin+Z1n2)*v para(inci, 1, 1) + (Rin-V)
Z1n2)/(Rin+Z1n2)*v para(inci,2,1));
v para(refl,1,1) = ((Z1n2-Rin)/(Rin+Z1n2)*v para(inci,1,1)+
2*Rin/(Rin+Z1n2)*v para(inci,2,1));
end
% with matching network
if (matched == 1)
v para(refl,2,1) = (2*Z1m/(Rin+Z1m)*v para(inci,1,1) + (Rin-x)
Z1m)/(Rin+Z1m)*v para(inci,2,1));
v para(refl, 1, 1) = ((Z1m-Rin) / (Rin+Z1m) * v para(inci, 1, 1) +
2*Rin/(Rin+Z1m)*v para(inci,2,1));
 vlmat(refl,1) = (Pm1*Cm*(2*Zsm2*Zsm3*vlmat(inci,1) + 2*Zsm1*Zsm3*vlmat(inci,2) + 2*Zsm2*vlmat(inci,2) + 2*
2*Zsm1*Zsm2*vlmat(inci,3)) + Rm11*vlmat(inci,1));
2*Zsm1*Zsm2*vlmat(inci,3))+ Rm33*vlmat(inci,3));
```

```
vlmat(refl, 2) = (Pm2*Cm * (2*Zsm2*Zsm3*vlmat(inci, 1) +
2*Zsm1*Zsm3*vlmat(inci,2)+2*Zsm1*Zsm2*vlmat(inci,3))+ Rm22*vlmat(inci,2));
v para(ref1,1,2)=(P1n2*Cn2*( 2*Zs2n2*Zs3n2*v para(inci,1,2)+
2*Zs1n2*Zs3n2*v para(inci,2,2)+2*Zs1n2*Zs2n2*v para(inci,3,2))+
R11n2*v para(inci,1,2));
v para(refl,3,2) = (P3n2*Cn2*(
2*Zs2n2*Zs3n2*v para(inci,1,2)+2*Zs1n2*Zs3n2*v para(inci,2,2)+2*Zs1n2*Zs2n2*v pa
ra(inci,3,2))+R33n2*v para(inci,3,2));
v para(refl, 2, 2) = (P2n2*Cn2*(
2*Zs2n2*Zs3n2*v para(inci,1,2)+2*Zs1n2*Zs3n2*v para(inci,2,2)+2*Zs1n2*Zs2n2*v pa
ra(inci,3,2))+R22n2*v para(inci,2,2));
v para(refl,1,3) = (P1n3*Cn3*(
2<sup>*</sup>Zs2n3*Zs3n3*v para(inci,1,3)+2*Zs1n3*Zs3n3*v para(inci,2,3)+2*Zs1n3*Zs2n3*v pa
ra(inci,3,3))+R11n3*v_para(inci,1,3));
v para(refl,3,3) = (P3n3*Cn3*(
2*Zs2n3*Zs3n3*v_para(inci,1,3)+2*Zs1n3*Zs3n3*v_para(inci,2,3)+2*Zs1n3*Zs2n3*v pa
ra(inci,3,3))+R33n3*v para(inci,3,3));
v para(refl, 2, 3) = (P2n3*Cn3*(
2*Zs2n3*Zs3n3*v para(inci,1,3)+2*Zs1n3*Zs3n3*v para(inci,2,3)+2*Zs1n3*Zs2n3*v pa
ra(inci,3,3))+R22n3*v para(inci,2,3));
v para(refl,1,4)=((Rout-
\overline{Z2}n3)/(Rout+Z2n3)*v para(inci,1,4)+(2*Z2n3)/(Rout+Z2n3)*v para(inci,2,4));
v \text{ para}(ref1, 2, 4) = ((2*Rout) / (Rout + Z2n3) * v para(inci, 1, 4) + (Z2n3 - Z2n3) * v para(inci, 1, 4) + (Z2n3 - Z2n3) * v para(inci, 1, 4) + (Z2n3 - Z2n3) * v para(inci, 1, 4) + (Z2n3 - Z2n3) * v para(inci, 1, 4) + (Z2n3 - Z2n3) * v para(inci, 1, 4) + (Z2n3 - Z2n3) * v para(inci, 1, 4) + (Z2n3 - Z2n3) * v para(inci, 1, 4) + (Z2n3 - Z2n3) * v para(inci, 1, 4) + (Z2n3 - Z2n3) * v para(inci, 1, 4) + (Z2n3 - Z2n3) * v para(inci, 1, 4) + (Z2n3 - Z2n3) * v para(inci, 1, 4) + (Z2n3 - Z2n3) * v para(inci, 1, 4) + (Z2n3 - Z2n3) * v para(inci, 1, 4) + (Z2n3 - Z2n3) * v para(inci, 1, 4) + (Z2n3 - Z2n3) * v para(inci, 1, 4) + (Z2n3 - Z2n3) * v para(inci, 1, 4) + (Z2n3 - Z2n3) * v para(inci, 1, 4) + (Z2n3 - Z2n3) * v para(inci, 1, 4) + (Z2n3 - Z2n3) * v para(inci, 1, 4) + (Z2n3 - Z2n3) * v para(inci, 1, 4) + (Z2n3 - Z2n3) * v para(inci, 1, 4) + (Z2n3 - Z2n3) * v para(inci, 1, 4) + (Z2n3 - Z2n3) * v para(inci, 1, 4) + (Z2n3 - Z2n3) * v para(inci, 1, 4) + (Z2n3 - Z2n3) * v para(inci, 1, 4) + (Z2n3 - Z2n3) * v para(inci, 1, 4) + (Z2n3 - Z2n3) * v para(inci, 1, 4) + (Z2n3 - Z2n3) * v para(inci, 1, 4) + (Z2n3 - Z2n3) * v para(inci, 1, 4) + (Z2n3 - Z2n3) * v para(inci, 1, 4) + (Z2n3 - Z2n3) * v para(inci, 1, 4) + (Z2n3 - Z2n3) * v para(inci, 1, 4) + (Z2n3 - Z2n3) * v para(inci, 1, 4) + (Z2n3 - Z2n3) * v para(inci, 1, 4) + (Z2n3 - Z2n3) * v para(inci, 1, 4) + (Z2n3 - Z2n3) * v para(inci, 1, 4) + (Z2n3 - Z2n3) * v para(inci, 1, 4) + (Z2n3 - Z2n3) * v para(inci, 1, 4) + (Z2n3 - Z2n3) * v para(inci, 1, 4) + (Z2n3 - Z2n3) * v para(inci, 1, 4) + (Z2n3 - Z2n3) * v para(inci, 1, 4) + (Z2n3 - Z2n3) * v para(inci, 1, 4) + (Z2n3 - Z2n3) * v para(inci, 1, 4) + (Z2n3 - Z2n3) * v para(inci, 1, 4) + (Z2n3 - Z2n3) * v para(inci, 1, 4) + (Z2n3 - Z2n3) * v para(inci, 1, 4) + (Z2n3 - Z2n3) * v para(inci, 1, 4) + (Z2n3 - Z2n3) * v para(inci, 1, 4) + (Z2n3 - Z2n3) * v para(inci, 1, 4) + (Z2n3 - Z2n3) * v para(inci, 1, 4) + (Z2n3 - Z2n3) * v para(inci, 1, 4) + (Z2n3 - Z2n3) * v para(inci, 1, 4) + (Z2n3 - Z2n3) * v para(inci, 1, 4) + (Z2n3 - Z
Rout) / (Rout+Z2n3) *v para(inci,2,4));
% connect
% without matching network
if (matched == 0)
v_para(inci,2,1) = v_para(refl,1,2);
v_para(inci,1,2)=v_para(refl,2,1);
v_para(inci,2,2)=v_para(refl,1,3);
v_para(inci,3,2)=v_para(refl,3,2);
v_para(inci,1,3)=v_para(refl,2,2);
v_para(inci,2,3)=v_para(refl,1,4);
v para(inci,3,3)=v_para(refl,3,3);
v para(inci,1,4)=v para(refl,2,3);
% with matching network
if (matched == 1)
v para(inci,2,1)=vlmat(refl,1);
vlmat(inci,1)=v para(refl,2,1);
vlmat(inci,2)=v_para(refl,1,2);
vlmat(inci,3)=vlmat(ref1,3);
v para(inci,1,2)=vlmat(refl,2);
v_para(inci,2,2)=v_para(refl,1,3);
v para(inci,3,2)=v para(ref1,3,2);
v_para(inci,1,3)=v_para(refl,2,2);
v para(inci,2,3)=v para(refl,1,4);
v_para(inci,3,3)=v_para(refl,3,3);
v para(inci,1,4)=v para(refl,2,3);
i active=(v para(inci,2,4)+v para(refl,2,4))/Rout;
% current to active layer
para inj=i active;
```

```
%return loss with matching
%for 1.1-6.6Ghz
%s11 n=s11 n+1;
%s11(s11 n,1)=para time;
%s11(s11 n,2)=vlmat(refl,1);
%return loss with matching
%at 6.6Ghz
s11 n=s11 n+1;
s11(s11 n,1)=para time;
s11(s11 n,2)=v para(refl,1,1);
% without matching
%s11 n=s11 n+1;
%s11(s11 n,1)=para time;
%s11(s11 n,2)=v para(refl,1,2);
%insertion loss
s21_n=s21_n+1;
s21(s21_n,1)=para_time;
s21(s21_n,2)=i_active;
res=0;
end
Calcarrdens
%This subprogram calculate the carrier rate equation
function res = calccarrdens(qtime,qinj,qss)
%DEFINE GLOBAL VARIABLES
global dirn maxsec scrf
% universal constants
global qelectron %electron charge
global planck
                %Planck's constant
                %speed of light
global co
% laser parameters
global neff
global fo %free-space lasing frequency
global beta %spontaneous emission coupling factor
               %wave impedance
global zp
               %carrier lifetime
global ts
                %attenuation
global attn
global ngrp
               %group index
               %cavity length
global len
               %gain compression factor
global gcomp
global r2
               %power facet reflectivities
global r1
                %power facet reflectivities
global no
                %transparency carrier density
```

```
%spatial gain per unit inversion
global aa
global cfn
                  %confinement factor
               %active region width
%active region thickness
global wid
global dthic
global nth %threshold carrier density
global mirlos %mirror loss
global linenfc %linewidth enhancement factor
global vol
                   %volume of the laser
global vol %volume of the laser
global auger %Auger recombination coefficient
global rad_1 %radiative recombination coefficient
global rad_0 %radiative recombination coefficient
global stim emis
% sampling time
global fsamp
                   %sampling frequency
global fnyq
                   %Nyquist frequency
global maxtime
global dl
                   %one section length
global dt
                   %time step
% sample carrier
global cstop
global cstart
% modulation
global i mod
                   %modulation current (1dBm max.power)
global freq rf %modulation frequency
global qnn
persistent qtrtm
persistent qtemp
persistent qtemp2
persistent avgqnn
persistent qitrtm
persistent qcnt
persistent qcnt2
persistent qtrigger
% initialisation
if (qtime == 0)
qtrtm=0;
qtemp=0;
qtemp2=0;
avgqnn=0;
qitrtm=0;
qcnt=0;
qcnt2=0;
gtrigger=0;
end
nn i=1.4e16;
% digitally filter with n-points, i.e. avg after n-points
qdfilpts=50;
%carrier rate equation
```

```
for qsec=1:maxsec
if (qnn(qsec) > no)
stim emis=1;
end
% without stimulated emission
if (stim emis == 0)
qnn(qsec)=(qnn(qsec)+dt*(qinj/(vol*qelectron)-(qnn(qsec)/ts+(rad 0-
rad 1*qnn(qsec))*qnn(qsec)^2+auger*qnn(qsec)^3)));
end
% stimulated emission-gain is taken into account
if (stim emis == 1)
qnn(qsec) = (qnn(qsec) + dt*(qinj/(vol*qelectron) - (qnn(qsec)/ts+(rad 0-
rad 1*qnn(qsec))*qnn(qsec)^2+auger*qnn(qsec)^3)-aa*(co/ngrp)*(qnn(qsec)-
no) *qss(qsec)));
end
% limit carrier extraction from ld
if (qnn(qsec) <= 0)
qnn(qsec)=nn i;
end
%longitudinal distribution of carrier density
if (qtime > maxtime)
if (mod(qtime, 200) == 0)
end
end
end
% output power at one facet corresponds to carrier density at that facet
qqnn=qnn (maxsec);
qqnn2=qnn(maxsec);
% car den variation with time at a specific section
if ((qtime >= cstart) && (qtime <= cstop))</pre>
qold=qtrigger;
qtrigger=sin(2*pi*freq rf*(qtime-cstart)*dt);
if ((qtrigger > 0) && (qold < 0))</pre>
qtrtm=0;
end
if (qtrigger == 0)
qtrtm=0;
end
qtrtm=qtrtm+1;
qcnt=qcnt+1;
qqnn=qtemp+qqnn;
qtemp=qqnn;
if (qcnt >= qdfilpts)
```

```
avgqnn=qqnn/qdfilpts;
qcnt=0;
qitrtm=qtrtm;
qtemp=0;
end
end
qcnt2=qcnt2+1;
qqnn2=qtemp2+qqnn2;
qtemp2=qqnn2;
if (qcnt2 >= qdfilpts)
avgcar=qqnn2/qdfilpts;
qcnt2=0;
qtold=qtime;
qtemp2=0;
end
res=0;
end
```

Calcphotdens

```
%This subprogram calculate photon density and output power
function res = calcphotdens(pinj,pgamma,ptime,pv)
persistent maxtsec
maxtsec=20000;
%DEFINE GLOBAL VARIABLES
global dirn maxsec scrf
% universal constants
global qelectron %electron charge
               %Planck's constant
global planck
                %speed of light
global co
% laser parameters
global neff %effective index
             %free-space lasing frequency %spontaneous emission coupling factor
global fo
global beta
global zp
               %wave impedance
global ts
               %carrier lifetime
global attn
               %attenuation
global ngrp
               %group index
global len
               %cavity length
global gcomp
               %gain compression factor
global r2
               %power facet reflectivities
global r1
               %power facet reflectivities
global no
               %transparency carrier density
global aa
               %spatial gain per unit inversion
global cfn
               %confinement factor
global wid
               %active region width
global dthic
               %active region thickness
global nth
               %threshold carrier density
```

```
global mirlos
global linenfc
                %mirror loss
                %linewidth enhancement factor
global vol
                %volume of the laser
% matrix notations
global refl
%reflected
global inci
               %incident
global bbb
               %backward
global aaa
                %forward
% sampling time
global fsamp
                 %sampling frequency
global fnyq
                %Nyquist frequency
global maxtime
global dl
                %one section length
global dt
                %time step
% modulation
global freq_rf
                %modulation current (1dBm max.power)
                %modulation frequency
% sample power
global pstop
global pstart
global findss 1
global rf11a
global rf11a_n
global rf11b
global rf11b_n
global pss
persistent maxtrtm
persistent trtm
persistent ptol
persistent temp
persistent temp2
persistent avgpower
persistent itrtm
persistent pcnt
persistent pcnt2
persistent told
persistent pppow
persistent pppow2
persistent swp
persistent nstba
persistent ptrigger
persistent avgpow
persistent favgp
%initialisation
if findss 1 == 0
   findss_1=1;
maxtrtm=0;
trtm=0;
ptol=0;
```

```
temp=0:
temp2=0;
avgpower=0;
itrtm=0;
pcnt=0;
pcnt2=0;
told=0;
pppow=0;
pppow2=0;
swp=1;
nstba=0;
ptrigger=0;
for iter=1:maxtsec
avgpow(iter)=0;
favgp(iter)=0;
end
end
% digitally filter with n-points, i.e. get avg of every n-points
dfilpts=50;
% find the photon density value in each section
for psec=1:maxsec
% gain compression factor is taken in account
if (pgamma(psec) ~= 0)
pss(psec) = ((pv(aaa, psec, inci)^2+
pv(bbb,psec,inci)^2)/(zp*planck*fo*(co/ngrp))*(exp(pgamma(psec))-
1)/pgamma(psec));
% without gain compression factor
elseif (pgamma(psec) == 0)
pss(psec) = ((pv(aaa, psec, inci)^2 + pv(bbb, psec, inci)^2 )/
(zp*planck*fo*(co/ngrp)));
end
end
% find instantaneous output power
ppow=(pv(bbb, 1, refl)^2*(1-r1)*wid*dthic/zp);
if (ptime > 0e-9/dt)
ptol=ptol+ppow;
if (ptime == maxtime)
pavg=(ptol/maxtime);
disp([ 'average output power per facet =' num2str(pavg) ])
end
end
```

```
% % collect instantaneous output power
% assign another variable name to ppow
pppow=ppow;
pppow2=ppow;
% the following routine is entered only if stated condition is satisfied
if ((ptime >= pstart) && (ptime <= pstop))</pre>
pold=ptrigger;
ptrigger=sin(2*pi*freq rf*(ptime-pstart)*dt);
if ((pold < 0) && (ptrigger > 0))
trtm=0;
swp=swp+1; %gives the total number of sweeps
end
if ((pold < 0) && (ptrigger == 0))</pre>
trtm=0;
swp=swp+1;
end
pcnt=pcnt+1;
pppow=temp+pppow;
temp=pppow;
% take average every n-points
if (pcnt >= dfilpts)
% stable-averaging algorithm
if ((swp > 2^{(nstba-1)}) & (swp < (2^{nstba+1}))
nstba=nstba;
elseif (swp >= (2^nstba+1))
nstba=nstba+1;
% only for first sweep
elseif (swp == 1)
nstba=nstba;
else
disp([ 'error with stable-averaging!' ])
disp([ 'swp=' num2str(swp) ])
disp([ 'nstba=' num2str(nstba) ])
error('error with stable-averaging!')
end
tinc=1;
trtm=trtm+tinc;
avgpow(trtm) = (avgpow(trtm) + (pppow/dfilpts-avgpow(trtm)) / (2^nstba));
pcnt=0;
temp=0;
if (trtm > maxtrtm)
maxtrtm=trtm;
end
end
end
```

```
% write to data file
if (ptime > pstop-dt)
for iter=1:maxtrtm
favgp(iter) = avgpow(iter);
rf11a n=rf11a n+1;
rflla(rflla n,1)=iter*dfilpts*dt; %stable averaged pulse
rf11a(rf11a n,2)=favgp(iter);
itrtm=iter;
end
end
%collect all optical pulses
pcnt2=pcnt2+1;
pppow2=temp2+pppow2;
temp2=pppow2;
if (pcnt2 >= dfilpts)
avgpower=pppow2/dfilpts;
pcnt2=0;
if ((ptime >= pstart) && (ptime <= pstop))</pre>
  rf11b_n=rf11b_n+1;
rf11b(rf11b n,1)=ptime*dt;
rf11b(rf11b n,2) = avgpower; %average over several optical pulses
end
told=ptime;
temp2=0;
end
res=0;
end
Matgain
%This subprogram estimate accurate gain curve
function res = matgain(efdcfo,efqeff,efa1,efa2,efa3,efa4)
% sampling time
global fsamp
global fnyq
efk1=sqrt(1/(4*efqeff^2+1));
efk2=sqrt(efdcfo^2/(4*efqeff^2*(fnyq-efdcfo)^2+efdcfo^2));
if (efk1 > efk2)
efa3=efk1;
efa4=1-efk1;
efk=efk2/efk1;
else
efa3=efk2;
efa4=1-efk2;
efk=efk1/efk2;
end
```

```
efa1=efk;
efa2=1-efk;
res=0;
end
```

Spontemissnoise

```
%This subprogram includes sponateous emission
function ress = spontemissnoise(snyl, snyc, sntotaly,
savgnn, na1, na3, na4, ntime, nsnn)
%DEFINE GLOBAL VARIABLES
global dirn maxsec scrf
% matrix notations
global refl
              %reflected
global inci
              %incident
global bbb
              %backward
global aaa
              %forward
% universal constants
global qelectron %electron charge
global planck
              %Planck's constant
global co
              %speed of light
% laser parameters
         %free-space lasing frequency
%spontaneous emission coupling factor
%wave impedance
global fo
global beta
global zp
global ts
              %carrier lifetime
global len
              %cavity length
global wid
              %active region width
              %active region thickness
global dthic
              %Auger recombination coefficient
global auger
global rad 1
              %radiative recombination coefficient
global rad 0
              %radiative recombination coefficient
% sampling time
global maxtime
global dl
              %one section length
global dt
               %time step
global spon 1
global nis
persistent nisc
persistent nisl
%initialisation
```

```
if spon 1 == 0
spon 1=1;
for nsec2=1:maxsec
nis(nsec2, inci) = 0;
nis(nsec2, refl) = 0;
nisc(nsec2,inci)=0;
nisc(nsec2, refl) = 0;
nisl(nsec2,inci)=0;
nisl(nsec2, refl) = 0;
end
end
if (ntime == maxtime)
disp(['spont emis pow per longi mode(empirical val) = '
num2str(dthic*wid*len*(planck*fo)*(beta*savgnn/ts))])
end
% inject spontaneous emission noise in each node
for nsec=1:maxsec
sdev(nsec) = sqrt(2*beta *(nsnn(nsec)/ts +(rad 0-
rad 1*nsnn(nsec))*nsnn(nsec)^2+auger*nsnn(nsec)^3)*planck*fo*maxsec/(zp*dl));
temp20=sdev(nsec);
nis(nsec,inci)=randn(1,1)*temp20; %spontaneous emission random generator
% with filter
% main line
nis(nsec,refl) = ((nis(nsec,inci)+2*snyc*nisc(nsec,inci)+2*snyl*nisl(nsec,inci))*(
1/sntotaly));
% capacitive stub line
nisc(nsec, refl) = ((nis(nsec, inci) + (2*snyc-
sntotaly)*nisc(nsec,inci)+2*snyl*nisl(nsec,inci))*(1/sntotaly));
% inductive stub line
nisl(nsec,refl) = ((nis(nsec,inci)+2*snyc*nisc(nsec,inci)+(2*snyl-
sntotaly) *nisl(nsec,inci)) * (1/sntotaly));
% waves on stub lines get reflected and becomes incident waves
% capacitive stub line
nisc(nsec,inci) = nisc(nsec,refl);
% inductive stub line
nisl(nsec, inci) = (-1.0d0) * nisl(nsec, refl);
end
ress=0;
```

Scattalgorithm

```
%This subprogram is needed for scattering algorithm
function res = scattalgorithm(scyc,scyl,sctotaly,sgain,sis1,stime)
%DEFINE GLOBAL VARIABLES
global maxsec
              %number of sections
% matrix notations
global refl
              %reflected
global inci
              %incident
global bbb
              %backward
global aaa
              %forward
% laser parameters
global zp
              %wave impedance
global attn
              %attenuation
% sampling time
global dl
              %one section length
              %time step
global dt
global sv
global svc
global svl
%output data
global pul1
global pul1 n
global pul2
global pul2 n
% scatter begin
maxsec=23;
for ssec=1:maxsec
% gain and attenuation implemented
% main transmission line (scatter fwd nodes)
sv(aaa,ssec,refl)=(( attn*(sgain(ssec))*sv(aaa,ssec,inci) +
2*scyc*svc(aaa,ssec,inci) + 2*scyl*svl(aaa,ssec,inci)) /sctotaly);
% flat response
sv(aaa, ssec, refl) = (sv(aaa, ssec, refl) + attn*sv(aaa, ssec, inci));
        endif
% scatter backwd nodes
```

```
sv(bbb,ssec,refl)=( (
attn*(sgain(ssec))*sv(bbb,ssec,inci)+2*scvc*svc(bbb,ssec,inci) +
2*scyl*svl(bbb,ssec,inci))/sctotaly);
% flat response
sv(bbb, ssec, refl) = (sv(bbb, ssec, refl) + attn*sv(bbb, ssec, inci));
           endif
% capacitive stub line
svc(aaa, ssec, refl) = ((sgain(ssec)*sv(aaa, ssec, inci) + (2*scyc-
sctotaly)*svc(aaa,ssec,inci)+2*scyl*svl(aaa,ssec,inci))/sctotaly);
svc(bbb, ssec, refl) = ((sgain(ssec)*sv(bbb, ssec, inci) + (2*scyc-
sctotaly) *svc(bbb, ssec,inci) +2*scyl*svl(bbb, ssec,inci))/sctotaly);
% inductive stub line
svl(aaa,ssec,refl) = ((
sgain(ssec)*sv(aaa,ssec,inci)+2*scyc*svc(aaa,ssec,inci)+(2*scyl-
sctotaly) *svl(aaa, ssec, inci))/sctotaly);
svl(bbb, ssec, refl) = ((
sgain(ssec)*sv(bbb,ssec,inci)+2*scyc*svc(bbb,ssec,inci)+(2*scyl-
sctotaly) *svl(bbb, ssec, inci))/sctotaly);
% inject spont emis nois at forward trav wave nodes; option: switch off
sv(aaa, ssec, refl) = (sv(aaa, ssec, refl) + sis1(ssec, refl) *zp*dl/2);
% inject spont emis nois at backward trav wave nodes
sv(bbb, ssec, refl) = (sv(bbb, ssec, refl) + sis1(ssec, refl) * zp*d1/2);
end
% investigate pulses
if((stime >= 10e-9/dt) && (stime < 11e-9/dt))
   pull n=pull n+1;
   pul1(pul1 n,1)=stime*dt;
   pull(pull n, 2) = sv(aaa, 1, refl);
if((stime >= 10e-9/dt) &&
                             (stime <= 40e-9/dt-4))
   pul2 n=pul2 n+1;
   pul2(pul2 n,1) = stime*dt;
   pul2(pul2 n,2) = sv(aaa, maxsec, refl);
end
res=0;
end
```

Connalgorithm

```
global dirn maxsec scrf
dirn=2;
maxsec=23; %number of sections
%maxsec=100;
scrf=2;
lf=1;
rf=2;
% matrix notations
global refl %reflected
global inci
                    %incident
global bbb
                    %backward
global aaa
                     %forward
% universal constants
global qelectron %electron charge
global planck
                      %Planck's constant
                      %speed of light
global co
% laser parameters
global neff %effective index
global fo %free-space lasing frequency
global beta %spontaneous emission coupling factor
global zp %wave impedance
                    %carrier lifetime
global ts
global attn
                    %attenuation
                    %group index
global ngrp
global len
                    %cavity length
                 %gain compression factor
%power facet reflectivities
global gcomp
global r2
                    %power facet reflectivities
global r1
                  %transparency carrier density
%spatial gain per unit inversion
%confinement factor
global no
global aa
global cfn
global wid
                    %active region width
                    %active region thickness
%threshold carrier density
global dthic
global nth
                    %mirror loss
global mirlos
global linenfc
%linewidth enhancement factor
%volume of the laser
global mirlos
                      %volume of the laser
global vol
% sampling time
global fsamp
                      %sampling frequency
global fnyq
                      %Nyquist frequency
global maxtime
qlobal dl
                      %one section length
global dt
                      %time step
% propagation
global omega
                      %angular frequency
global pbeta
                      %propagation constant
% sample power
global pstop
global pstart
global connect 1
global sv
global svc
global svl
```

```
persistent cstb
% begin connection between nodes
for csec=1:maxsec
% notation for adjacent node
secp1=csec+1;
secn1=csec-1;
% initialisation
if connect 1 == 0
   connect 1=1;
cstb(lf,inci)=0;
               %left facet
cstb(lf,refl)=0;
cstb(rf,inci)=0; %right facet
cstb(rf,refl)=0;
end
% instantaneous phase length
phlen=(cfn*(-linenfc*co*aa/(4*pi*fo))*(cavgnn-nth)*len/ngrp);
% 1st case: impedance of the open circuit stub (capacitive stub)
if (tan(pbeta*phlen) > 0)
czs=zp*tan(pi*fo*dt)/tan(pbeta*phlen);
%2nd case: impedance of the short circuit stub (inductive stub).
if (tan(pbeta*phlen) < 0)</pre>
czs=-zp/(tan(pi*fo*dt)*tan(pbeta*phlen));
end
%chirp is taken into account
if (tan(pbeta*phlen) ~= 0)
if (csec == 1)
% forward waves
sv(aaa, csec, inci) = (1/(czs+zp)*(sqrt(r1)*(czs-zp)*sv(bbb, csec, refl)+
2*sqrt(r1)*zp*cstb(lf,inci)));
cstb(lf, refl) = (1/(czs+zp)*(2*czs*sv(bbb, csec, refl) + (zp-czs)*cstb(lf, inci)));
else
sv(aaa, csec, inci) = sv(aaa, secn1, refl);
end
% backward waves
if (csec == maxsec)
sv(bbb, csec, inci) = (1/(czs+zp)*(sqrt(r2)*(czs-zp)*sv(aaa, csec, refl)+
2*sqrt(r2)*zp*cstb(rf,inci)));
cstb(rf, refl) = (1/(czs+zp)*(2*czs*sv(aaa, csec, refl) + (zp-czs)*cstb(rf, inci)));
sv(bbb, csec, inci) = sv(bbb, secp1, refl);
end
end
```

```
%without chirp consideration
if (tan(pbeta*phlen) == 0)
% forward waves
if (csec == 1)
sv(aaa,csec,inci) = sqrt(r1) *sv(bbb,csec,ref1); % reflection at left facet
else
sv(aaa,csec,inci) = sv(aaa,secn1,refl);
end
% backward waves
if (csec == maxsec)
sv(bbb,csec,inci)=sqrt(r2)*sv(aaa,csec,refl); % reflection at right facet
else
sv(bbb, csec, inci) = sv(bbb, secp1, refl);
end
end
% capacitive stub
svc(aaa,csec,inci) = svc(aaa,csec,refl);
svc(bbb, csec, inci) = svc(bbb, csec, refl);
% inductive stub
svl(aaa, csec, inci) = (-1) *svl(aaa, csec, refl);
svl(bbb, csec, inci) = (-1) *svl(bbb, csec, refl);
% stub-attenuator
if (tan(pbeta*phlen) > 0)
cstb(lf,inci)=cstb(lf,refl);
cstb(rf,inci)=cstb(rf,refl);
elseif (tan(pbeta*phlen) < 0)</pre>
cstb(lf,inci) = -cstb(lf,refl);
cstb(rf,inci) =-cstb(rf,refl);
else
cstb(lf,inci)=0;
cstb(rf,inci)=0;
end
end
res=0;
end
Graphs
%This program outputs graphs from the txt file
a1=1;
figure (a1);
fig=10;
           %choose required figure by changing number
%shows input signal to laser cavity
if fig==1
data=dlmread('injpr1.txt');
size(data)
plot(data(:,1), data(:,2))
print(a1,['injpr1.png'],'-dpng');
```

```
end
if fig==2
data=dlmread('injpr2.txt');
size(data)
plot(data(:,1), data(:,2))
print(a1,['injpr2.png'],'-dpng');
%shows return loss S11 for 1.1GHz
if fig==3
N=2^10;
fl1=1.1*10^9;
frq1=[-N/2:N/2-1]/N*(1e-9)*fl1+(fl1*(1e-9));
data1=dlmread('s111.txt');
fftdata1=abs(fft(data1(:,2),N)); % take data only from2d column
fftdatalog1=20*log10(fftdata1);
fl2=6.6*10^9;
frq2=[-N/2:N/2-1]/N*(1e-9)*fl2+(fl2*(1e-9));
data2=dlmread('s116.txt');
fftdata2=abs(fft(data2(:,2),N)); % take data only from2d column
fftdatalog2=20*log10(fftdata2);
plot(frq1,fftdatalog1,frq2,fftdatalog2);
print(a1,['s111fftlog.png'],'-dpng');
end
%shows gain switched optical pulses for 1.1, 2.2, 6.6 GHz
if fig==4
rf11b1=dlmread('rf11b1.txt');
rf11b2=dlmread('rf11b2.txt');
rf11b6=dlmread('rf11b6.txt');
size(rf11b1)
plot(rf11b1(:,1),rf11b1(:,2),'-r',rf11b2(:,1),rf11b2(:,2),'--
b',rf11b6(:,1),rf11b6(:,2),'-g' )
print(a1,['rf11b.png'],'-dpng');
end
%shows stable average pulse for mathced and unmatched case for 2.2 GHz
if fig==5
rf11am=dlmread('rf11am.txt');
rf11anm=dlmread('rf11anm.txt');
size(rf11a)
plot(rf11am(:,1),rf11am(:,2),'-b',rf11anm(:,1),rf11anm(:,2),'--g')
print(a1,['rf11a.png'],'-dpng');
end
%shows stable average pulse for mathced and unmatched case for 2.2 GHz
if fig==6
rf11b2GHzbeta0=dlmread('rf11b2GHzbeta0.txt');
rf11b2GHzbeta5=dlmread('rf11b2GHzbeta5.txt');
size(rf11b2GHzbeta0)
```

plot(rf11b2GHzbeta0(:,1),rf11b2GHzbeta0(:,2),'r',rf11b2GHzbeta5(:,1),rf11b2GHzbeta5(:,2),'-b')

print(a1,['rf11b2GHzbeta0.png'],'-dpng');

end

```
%shows optical and RF pulses biased at 1.3*Ith in time domain
if fig==7
data=dlmread('pul1.txt');
size(data)
plot(data(:,1), data(:,2))
print(a1,['pul1.png'],'-dpng');
end
if fig==8
N=2^15;
fl=1.1*10^9;
frq=[-N/2:N/2-1]/N*(1e-9)*fl+(fl*(1e-9));
data=dlmread('pul1.txt');
fftdata=abs(fft(data(:,2), N)); % take data only from2d column
fftdatalog=10*log10(fftdata);
plot(frq,fftdatalog);
print(a1,['pulllog.png'],'-dpng');
end
%shows optical and RF pulses when gain switched (1dBm RF power)
if fig==9
data=dlmread('pul2.txt');
size(data)
plot(data(:,1), data(:,2))
print(a1,['pul2.png'],'-dpng');
end
if fig==10
N=2^15;
fl=1.1*10^9;
frq=[-N/2:N/2-1]/N;
frq=[-N/2:N/2-1]/N*(1e-9)*fl+(fl*(1e-9));
data=dlmread('pul2.txt');
fftdata=abs(fft(data(:,2), N)); % take data only from2d column
fftdatalog=10*log10(fftdata);
plot(frq,fftdatalog);
print(a1,['pul2log.png'],'-dpng');
%shows transient response for 1.1GHz for mathced and unmatched cases
%if fig==4
%data=dlmread('s211.txt');
%data=dlmread('s216.txt');
%size(S21)
%plot(s211(:,1),s211(:,2),s216(:,1),s216(:,2))
%plot(data(:,1),data(:,2))
%print(a1,['s21.png'],'-dpng');
%end
%This program outputs graphs from the txt file
a1=1;
figure (a1);
         %choose required figure by changing number
```

```
%shows input signal to laser cavity
if fig==1
data=dlmread('injpr1.txt');
size(data)
plot(data(:,1),data(:,2))
print(a1,['injpr1.png'],'-dpng');
end
if fig==2
data=dlmread('injpr2.txt');
size(data)
plot(data(:,1),data(:,2))
print(a1,['injpr2.png'],'-dpng');
end
%shows return loss S11 for 1.1GHz
if fig==3
N=2^10;
fl1=1.1*10^9;
frq1=[-N/2:N/2-1]/N*(1e-9)*fl1+(fl1*(1e-9));
data1=dlmread('s111.txt');
fftdata1=abs(fft(data1(:,2),N)); % take data only from2d column
fftdatalog1=20*log10(fftdata1);
fl2=6.6*10^9;
frq2=[-N/2:N/2-1]/N*(1e-9)*f12+(f12*(1e-9));
data2=dlmread('s116.txt');
fftdata2=abs(fft(data2(:,2),N)); % take data only from2d column
fftdatalog2=20*log10(fftdata2);
plot(frq1,fftdatalog1,frq2,fftdatalog2);
print(a1,['s111fftlog.png'],'-dpng');
end
%shows gain switched optical pulses for 1.1, 2.2, 6.6 GHz
if fig==4
rf11b1=dlmread('rf11b1.txt');
rf11b2=dlmread('rf11b2.txt');
rf11b6=dlmread('rf11b6.txt');
size(rf11b1)
plot(rf11b1(:,1),rf11b1(:,2),'-r',rf11b2(:,1),rf11b2(:,2),'--
b',rf11b6(:,1),rf11b6(:,2),'-g')
print(a1,['rf11b.png'],'-dpng');
%shows stable average pulse for mathced and unmatched case for 2.2 GHz
if fig==5
rf11am=dlmread('rf11am.txt');
rfllanm=dlmread('rfllanm.txt');
size(rf11a)
plot(rf11am(:,1),rf11am(:,2),'-b',rf11anm(:,1),rf11anm(:,2),'--g')
print(a1,['rf11a.png'],'-dpng');
%shows optical and RF pulses biased at 1.3*Ith in time domain
if fig==6
data=dlmread('pul1.txt');
size(data)
plot(data(:,1), data(:,2))
```

```
print(a1,['pul1.png'],'-dpng');
end
if fig==7
N=2^15;
fl=1.1*10^9;
frq=[-N/2:N/2-1]/N*(1e-9)*fl+(fl*(1e-9));
data=dlmread('pul1.txt');
fftdata=abs(fft(data(:,2), N)); % take data only from2d column
fftdatalog=10*log10(fftdata);
plot(frq,fftdatalog);
print(a1,['pulllog.png'],'-dpng');
end
%shows optical and RF pulses when gain switched (1dBm RF power) with beta=0
if fig==8
N=2^15;
fl=1.1*10^9;
frq=[-N/2:N/2-1]/N;
frq=[-N/2:N/2-1]/N*(1e-9)*fl+(fl*(1e-9));
data=dlmread('pul2beta0.txt');
fftdata=abs(fft(data(:,2), N)); % take data only from2d column
fftdatalog=10*log10(fftdata);
plot(frq,fftdatalog);
print(a1,['pul2log.png'],'-dpng');
end
%shows optical and RF pulses when gain switched (1dBm RF power) with
%beta=5.6
if fig==9
N=2^15;
fl=1.1*10^9;
frq=[-N/2:N/2-1]/N;
frq=[-N/2:N/2-1]/N*(1e-9)*fl+(fl*(1e-9));
data=dlmread('pul2beta5.txt');
fftdata=abs(fft(data(:,2), N)); % take data only from2d column
fftdatalog=10*log10(fftdata);
plot(frq,fftdatalog);
print(a1,['pul2log.png'],'-dpng');
end
%shows optical and RF pulses when gain switched (1dBm RF power)
if fig==10
data=dlmread('pul2.txt');
size(data)
plot(data(:,1),data(:,2))
print(a1,['pul2.png'],'-dpng');
end
if fig==11
N=2^15;
fl=1.1*10^9;
frq=[-N/2:N/2-1]/N;
frq=[-N/2:N/2-1]/N*(1e-9)*fl+(fl*(1e-9));
data=dlmread('pul2.txt');
fftdata=abs(fft(data(:,2), N)); % take data only from2d column
```